NEUROSCIENCE

An autophagy-related protein Becn2 regulates cocaine reward behaviors in the dopaminergic system

Yoon-Jin Kim[1]*, Qingyao Kong[2]*, Soh Yamamoto[1,3], Kenta Kuramoto[1], Mei Huang[4], Nan Wang[1,5], Jung Hwa Hong[1], Tong Xiao[1], Beth Levine[6†], Xianxiu Qiu[1,7‡], Yanxiang Zhao[7], Richard J. Miller[8], Hongxin Dong[4], Herbert Y. Meltzer[4], Ming Xu[2], Congcong He[1§]

Drug abuse is a foremost public health problem. Cocaine is a widely abused drug worldwide that produces various reward-related behaviors. The mechanisms that underlie cocaine-induced disorders are unresolved, and effective treatments are lacking. Here, we found that an autophagy-related protein Becn2 is a previously unidentified regulator of cocaine reward behaviors. *Becn2* deletion protects mice from cocaine-stimulated locomotion and reward behaviors, as well as cocaine-induced dopamine accumulation and signaling, by increasing presynaptic dopamine receptor 2 (D2R) autoreceptors in dopamine neurons. Becn2 regulates D2R endolysosomal trafficking, degradation, and cocaine-induced behaviors via interacting with a D2R-bound adaptor GASP1. Inactivating Becn2 by upstream autophagy inhibitors stabilizes striatal presynaptic D2R, reduces dopamine release and signaling, and prevents cocaine reward in normal mice. Thus, the autophagy protein Becn2 is essential for cocaine psychomotor stimulation and reward through regulating dopamine neurotransmission, and targeting Becn2 by autophagy inhibitors is a potential strategy to prevent cocaine-induced behaviors.

INTRODUCTION

Control of drug abuse and addiction has emerged as one of the major medical and social challenges of our time. Cocaine is one of the most widely abused recreational drugs throughout the world. Although many efforts have been made to understand cocaine abuse and addiction, the mechanisms that underlie these effects are not fully understood, and therapeutic strategies for preventing and treating cocaine-induced behaviors are lacking (*1*). Mesolimbic dopamine (DA) signaling has been reported to play an important role in the regulation of cocaine-associated reward and motivation (*2*), and its dysregulation is implicated in a variety of neurological/neuropsychiatric disorders such as drug addiction, depression, and schizophrenia. The neurotransmitter DA is released from axons of midbrain dopaminergic neurons located in the ventral tegmental area (VTA) projecting to the nucleus accumbens (NAc; or ventral striatum) and the prefrontal cortex (*3*). The psychostimulant drug cocaine elevates synaptic DA levels in the NAc by blocking DA reuptake by the DA transporter (DAT). The resulting synaptic DA surge increases postsynaptic activation of DA receptors, producing psychomotor stimulation after acute exposure and behavioral sensitization, craving, and reward-related behaviors after repeated usage (*2*, *4*, *5*).

DA release is negatively regulated by presynaptic striatal DA receptor 2 (D2R) in dopaminergic neurons, a G protein–coupled receptor (GPCR) that functions as an autoreceptor (*6*–*8*) and regulates many aspects of cellular and behavioral responses to cocaine exposure (*9*–*11*). On one hand, aberrant D2R function in the brain increases the risk of substance abuse (*12*–*14*), and on the other hand, D2R is substantially down-regulated in addicted brain (*5*, *15*, *16*). Mice in which the D2R autoreceptors are deleted showed supersensitivity to cocaine, including increased locomotor stimulation and conditioned place preference (CPP) for cocaine (*11*). Since elevation in synaptic DA concentration in the NAc is essential for exerting cocaine's effects in locomotor control, behavioral sensitization, and reward seeking, understanding the factors controlling DA release is important for preventing cocaine abuse, and reducing DA release and elevating D2R availability may be an effective potential strategy for treating cocaine-associated behaviors. However, the in vivo mechanism responsible for the down-regulation of D2R in response to drugs of abuse remains mysterious.

In this study, we discover that Becn2/Beclin 2, an autophagy-related protein and a Beclin/Becn family member that forms a complex with the autophagy-inducing class III phosphatidylinositol 3-kinase (PtdIns 3-kinase) Vps34 (*17*, *18*), genetically links the physiological and behavioral effects of cocaine to the autophagy pathway. Autophagy is an essential lysosomal degradation pathway induced by stress, such as starvation (*19*) and exercise (*20*). During autophagy, autophagosomes enwrap and deliver damaged or unnecessary cargos to lysosomes for breakdown and nutrient recycling. Although accumulating evidence indicates that autophagy proteins are implicated in a variety of diseases, such as type 2 diabetes, neurodegeneration, and cancer (*21*–*23*), whether and how they play a role in drug seeking and abuse are essentially unknown.

High dosages of cocaine cause cytotoxicity and have been reported to induce autophagy and autophagic cell death in cultured neurons and astrocytes (*24*, *25*). However, whether there is a link between autophagy and the behavioral responses of cocaine in vivo and the underlying basis is not known. Ablation of an autophagy gene *Atg7*

[1]Department of Cell and Developmental Biology, Feinberg School of Medicine, Northwestern University, Chicago, IL 60611, USA. [2]Department of Anesthesia and Critical Care, The University of Chicago, Chicago, IL 60637, USA. [3]Department of Microbiology, Sapporo Medical University School of Medicine, Sapporo 060-8556, Japan. [4]Department of Psychiatry and Behavioral Sciences, Feinberg School of Medicine, Northwestern University, Chicago, IL 60611, USA. [5]Key Laboratory of Industrial Microbiology, Ministry of Education and Tianjin City, College of Biotechnology, Tianjin University of Science and Technology, Tianjin 300457, China. [6]Departments of Internal Medicine and Microbiology, Howard Hughes Medical Institute, University of Texas Southwestern Medical Center, Dallas, TX 75390, USA. [7]Department of Applied Biology and Chemical Technology, The Hong Kong Polytechnic University, Hung Hom, Hong Kong, China. [8]Department of Pharmacology, Feinberg School of Medicine, Northwestern University, Chicago, IL 60611, USA.
*These authors contributed equally to this work.
†Deceased.
‡Present address: Guangdong Medical University, Dongguan 523808, China.
§Corresponding author. Email: congcong.he@northwestern.edu

specifically in DA neurons was previously reported to cause a slight increase in baseline DA secretion (without cocaine injection) (*26*); yet, whether the increase is physiologically important or whether it would lead to behavioral changes in response to psychostimulants has not been investigated.

Here, we use a number of global and conditional knockout (KO) and knock-in (KI) mouse models to demonstrate the role and mechanism of an autophagy protein Becn2 and autophagy inhibitors in cocaine-evoked physiological responses and reward behaviors via DA regulation. We reveal that defects in Becn2 prevent cocaine-induced behavioral responses, reduce cocaine-induced extracellular DA accumulation, and increase presynaptic D2R levels in the NAc, suggesting that the autophagy protein Becn2 is a pivotal player in regulating cocaine-induced behaviors by degrading D2R autoreceptors and regulating DA release in DA neurons. In addition, we provide evidence that Becn2 is a potential therapeutic target in the prevention of cocaine responses and propose a model in which targeting Becn2 by upstream autophagy inhibitors prevents cocaine-induced extracellular DA accumulation and drug-reward behaviors. Our study demonstrates how an autophagy-related protein regulates DA signaling and behavioral responsiveness to cocaine and suggests the neurotherapeutic potential of using autophagy modulators to prevent seeking and abuse of psychoactive substances.

RESULTS

Haplodeletion of *Becn2*, but not *Becn1*, prevents cocaine psychomotor stimulation and reward behaviors

To study the function of Beclin/Becn family members in the regulation of cocaine-induced behaviors, we used heterozygous KO mouse models of *Becn1* and *Becn2* as tools in behavioral studies, because homozygous KO of either *Becn1* or *Becn2* causes complete or partial embryonic lethality (*17*, *27*). We first analyzed their behavioral responsiveness to acute cocaine injection, using cocaine-induced locomotor stimulation as a readout. We found that *Becn2*$^{+/-}$ KO mice have markedly lower locomotor activity after cocaine treatment (15 mg/kg) than wild-type (WT) littermates in open-field tests (Fig. 1A). In contrast, heterozygous KO of *Becn1* does not significantly affect cocaine-stimulated locomotion (Fig. 1A). To systematically characterize whether Becn2 regulates the pharmacological effects of cocaine, we analyzed the dose-dependent response to cocaine of *Becn2*$^{+/-}$ KO mice and WT littermates in open-field tests at a lower dose (5 mg/kg) and a higher dose (30 mg/kg) of cocaine. In addition to cocaine (15 mg/kg), we found that *Becn2*$^{+/-}$ KO mice also showed reduced locomotor activity induced by a high cocaine concentration (30 mg/kg) (fig. S1A). Further, we did not detect changes in Becn1 expression in *Becn2*$^{+/-}$ KO mice (fig. S1B). Thus, together, these data suggest that Becn2, but not another autophagy-related Beclin protein Becn1, plays an important role in regulating behavioral responses to acute cocaine exposure.

We next analyzed the function of Becn2 in reward behaviors induced by repeated exposure to cocaine. The CPP test, although not sensitive to dose-response studies, is widely used to measure reward learning. We found that compared with WT littermates, *Becn2*$^{+/-}$ KO mice spend less time in the cocaine-paired environment after 8 days of alternate cocaine and phosphate-buffered saline (PBS) injections (Fig. 1B), suggesting that Becn2 is also essential for cocaine-induced reward learning. Notably, CPP to food, a nondrug reward, is not affected in *Becn2*$^{+/-}$ KO mice (fig. S1C), suggesting that *Becn2* haplodeletion does not cause an overall learning deficit, and reduced cocaine CPP in *Becn2*$^{+/-}$ KO mice is not caused by defective learning.

The rodent intravenous self-administration (IVSA) models voluntary drug intake in humans and is an ideal model for studying voluntary drug seeking and taking (*28*). Since haplodeletion of *Becn2* reduces CPP to cocaine, we asked whether Becn2 regulates self-administration of cocaine in vivo to model human addiction characterized by voluntary and escalated cocaine intake. Following 10 days of IVSA training (0.6 mg/kg per infusion of cocaine dose), *Becn2*$^{+/-}$ KO mice showed significantly lower active nose pokes and infusion numbers and self-administered less cocaine than WT controls (Fig. 1C). Dose-response studies also showed that *Becn2*$^{+/-}$ KO mice exhibited a tendency of lower active nose pokes and cocaine intake than WT controls after IVSA training with two different cocaine doses (0.1 and 1.0 mg/kg per infusion) (Fig. 1D). These results suggest that Becn2 depletion decreases acquisition of cocaine-taking behaviors, which is consistent with the findings in CPP and locomotor activity. Thus, we concluded that Becn2 is essential to regulate behavioral responsiveness to both acute and repeated cocaine exposure.

Haplodeletion of *Becn2* reduces cocaine-induced extracellular accumulation of DA but not other neurotransmitters

To study the mechanism through which Becn2 regulates behavioral responses to cocaine, we performed ultraperformance liquid chromatography (UPLC) profiling for cocaine-amplified, Becn2-regulated neurotransmitters in the NAc and cortex of WT and *Becn2*$^{+/-}$ KO mice following microdialysis. We found that cocaine-induced extracellular accumulation of DA (both the exact quantity and the percentage of baseline concentration; Fig. 2A), but not other neurotransmitters such as acetylcholine (ACh), serotonin (5-hydroxytryptamine), and glutamate (fig. S2A), is blocked in the NAc of *Becn2*$^{+/-}$ KO mice. Extracellular levels of DA metabolites in the NAc, such as DOPAC (3,4-dihydroxyphenylacetic acid) and HVA (homovanillic acid), were not regulated by cocaine or Becn2 either (fig. S2B). In addition, in the prefrontal cortex, there is also a significant reduction in cocaine-amplified release of DA in *Becn2*$^{+/-}$ KO mice compared to WT littermates (fig. S2C). Together, these data suggest that haplodeletion of *Becn2* limits DA release to the NAc and cortex, which becomes evident following exposure to cocaine.

This finding is further corroborated by our biochemical data on cocaine-induced DA signaling. Increased synaptic DA activates the postsynaptic mitogen-activated protein kinase (MAPK) pathway, including MAPK kinase 1/2 (MEK1/2) and extracellular signal–regulated kinase 1/2 (ERK1/2) cascades (*29*). We found that acute cocaine treatment induces MEK and ERK phosphorylation (activation) in WT mice but fails to do so in *Becn2*$^{+/-}$ KO mice in both the NAc and the whole striatum region (Fig. 2B and fig. S2D). In addition, we found that phosphorylation of CREB (adenosine 3′,5′-monophosphate response element–binding protein) at Ser^{133}, a transcription factor playing an important role in addiction and a downstream signal of the synaptic activity and MAPK pathway (*30*, *31*), is also blunted in the NAc of *Becn2*$^{+/-}$ KO mice after cocaine treatment, compared to WT littermates (Fig. 2C). Note that *Becn2*$^{+/-}$ KO mice have a comparable anxiety level as WT mice, analyzed by elevated zero maze (fig. S3), which is consistent with the normal basal DA levels and signaling in their NAc without cocaine treatment (Fig. 2). These data suggest that *Becn2* haplodeletion reduces cocaine-induced kinase activation, supporting a role of Becn2 in the cocaine-induced extracellular accumulation of DA. Thus, we

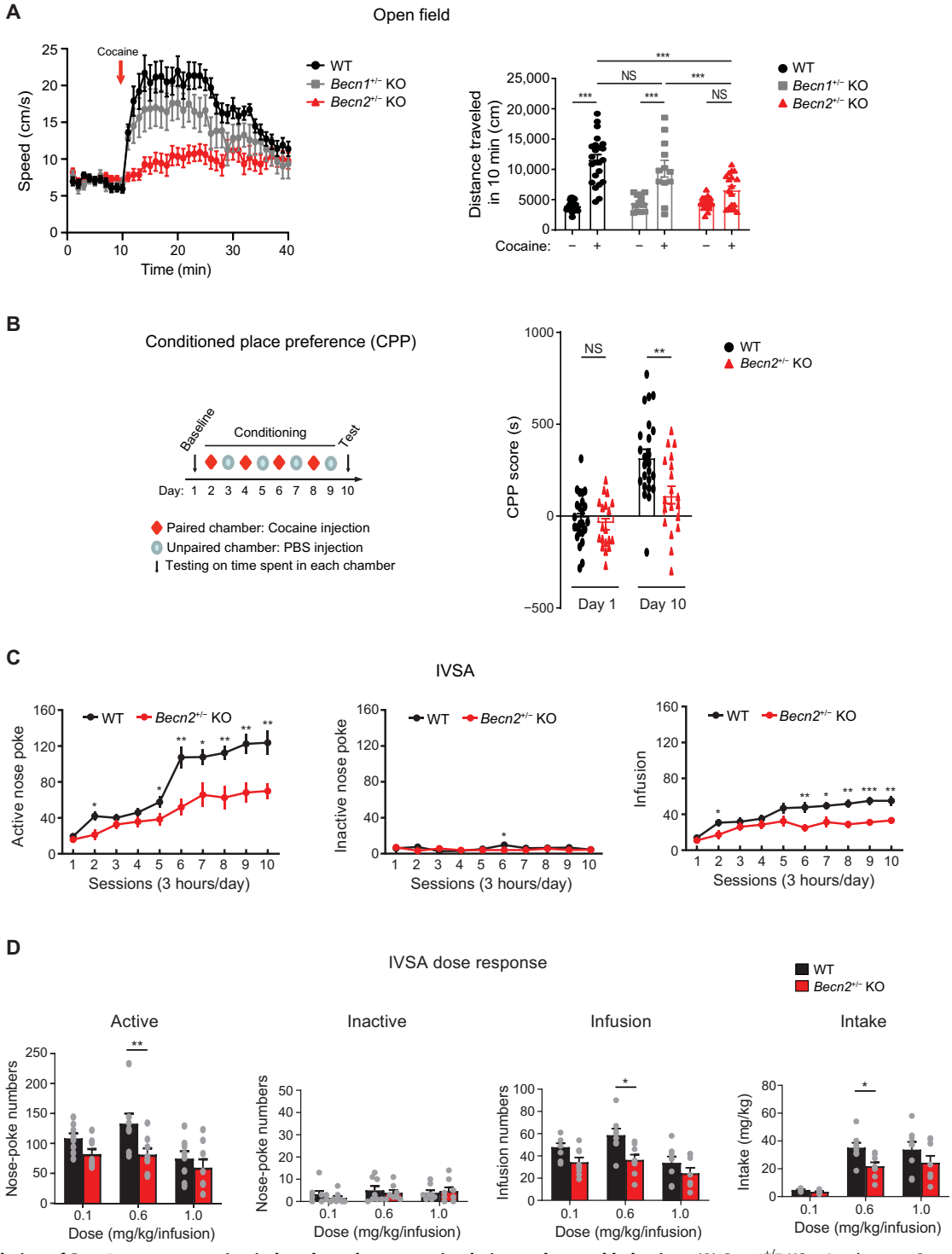

Fig. 1. Haplodeletion of *Becn2* prevents cocaine-induced psychomotor stimulation and reward behaviors. (**A**) $Becn2^{+/-}$ KO mice, but not $Becn1^{+/-}$ KO mice, are protected from cocaine-stimulated locomotion. Left: Locomotor activity of WT, $Becn1^{+/-}$ KO, and $Becn2^{+/-}$ KO mice monitored by open-field test upon intraperitoneal injection of cocaine (15 mg/kg; arrow). Right: Quantification of distance traveled in 10 min before and after cocaine treatment. WT, $N = 23$; $Becn1^{+/-}$ KO, $N = 12$; $Becn2^{+/-}$ KO, $N = 18$. (**B**) $Becn2^{+/-}$ KO mice show reduced CPP to repeated cocaine dosage. WT and $Becn2^{+/-}$ KO mice received cocaine (15 mg/kg) or PBS injection alternately for 8 days (conditioning), and their time spent in the paired (cocaine-injecting) chamber and the unpaired (PBS-injecting) chamber was recorded (CPP test). The CPP score is calculated as the difference in time (seconds) spent in the paired and unpaired chambers. WT, $N = 24$; $Becn2^{+/-}$ KO, $N = 19$. (**C**) Cocaine IVSA in $Becn2^{+/-}$ KO and WT control mice. The cocaine dose used was 0.6 mg/kg per infusion. Active nose-poke, inactive nose-poke, and infusion numbers were recorded in 3-hour sessions each training day. $N = 12$ per group. (**D**) IVSA dose response in $Becn2^{+/-}$ KO and WT mice. Cocaine doses used were 0.1, 0.6, and 1 mg/kg per infusion. Numbers of active nose poke, inactive nose poke, and cocaine infusion and the amount of cocaine intake were recorded in 3-hour sessions each training day. Data represent means ± SEM. $N = 8$ per group. $^{*}P < 0.05$; $^{**}P < 0.01$; $^{***}P < 0.001$; NS, not significant.

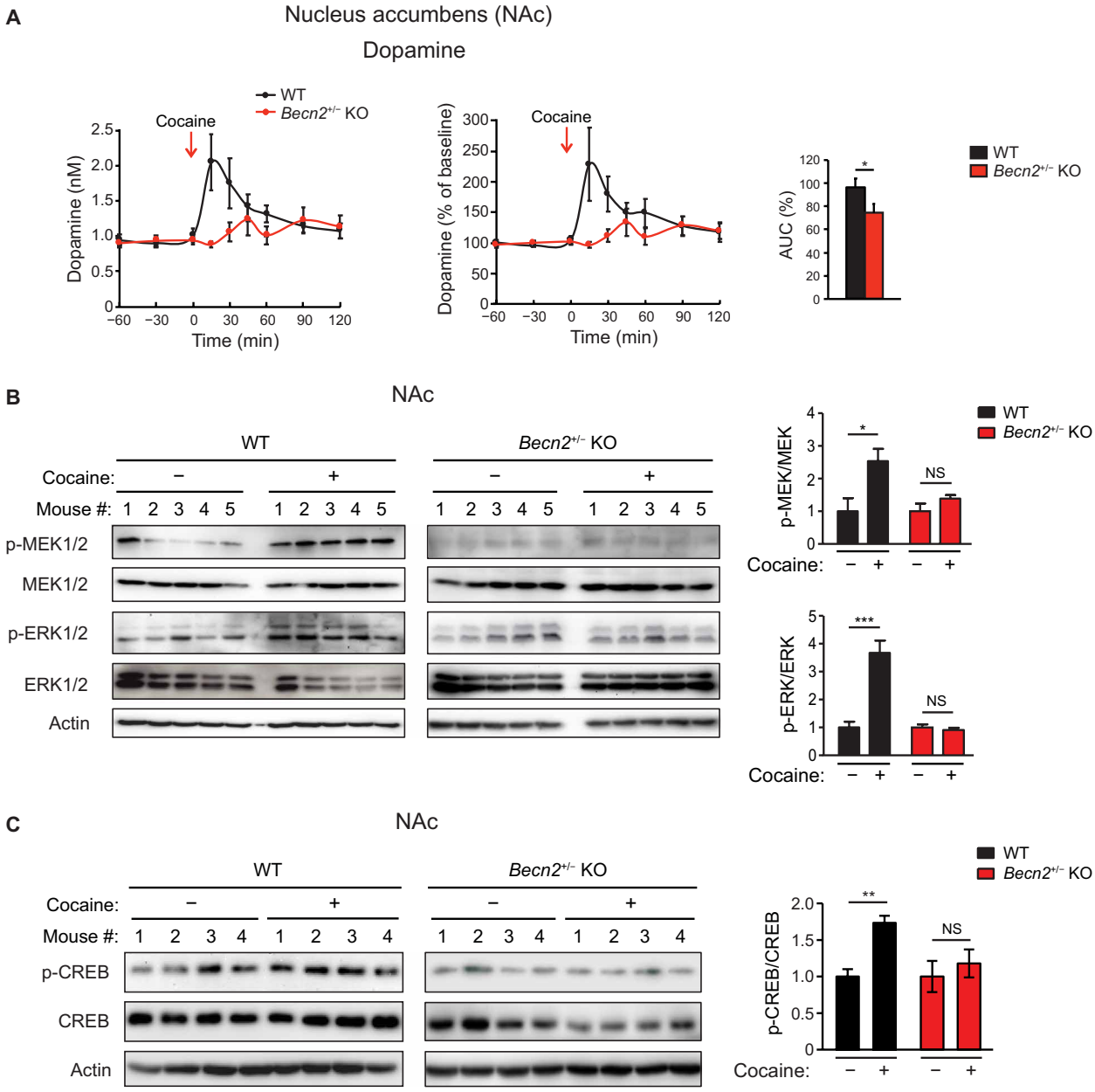

Fig. 2. Haplodeletion of *Becn2* prevents DA release and signaling in response to cocaine. (**A**) Microdialysis analyses showing concentration and percentage of baseline of DA in NAc of WT and *Becn2* KO mice at the indicated time points before and after cocaine injection. Area under the curve (AUC) is quantified for 120 min after cocaine injection. WT, $N = 9$; *Becn2*$^{+/-}$ KO, $N = 8$. (**B**) Cocaine-induced kinase activation is blunted in *Becn2*$^{+/-}$ KO mouse brain. Western blot analyses and quantification of cocaine-induced MEK and ERK phosphorylation in the NAc of WT and *Becn2*$^{+/-}$ KO mouse brain 15 min after cocaine (15 mg/kg) or vehicle intraperitoneal injection. $N = 5$ mice. (**C**) Cocaine-induced CREB phosphorylation is blunted in *Becn2*$^{+/-}$ KO mouse brain. Western blot analyses and quantification of cocaine-induced CREB phosphorylation in the NAc of WT and *Becn2*$^{+/-}$ KO mouse brain 15 min after cocaine (15 mg/kg) or vehicle intraperitoneal injection. $N = 4$ mice. $^{*}P < 0.05$; $^{**}P < 0.01$; $^{***}P < 0.001$.

conclude that Becn2 regulates cocaine-amplified DA release and DA signaling in the NAc.

Becn2 functions in DA neurons to regulate cocaine responses

To further map the neuronal populations in which Becn2 regulates cocaine responses and DA release, we generated a floxed *Becn2* KO (*Becn2*$^{flox/flox}$) mouse line to study its neuronal-specific function (fig. S4A). On one hand, we deleted *Becn2* specifically in DA neurons during adulthood, by delivering the DA neuron–specific TH (tyrosine hydroxylase) promoter Cre into the VTA of *Becn2*$^{flox/flox}$ mice via adeno-associated virus 2/9 (AAV2/9) by stereotaxic microinjection (fig. S4, B and C). We found that similar to global *Becn2*$^{+/-}$ KO mice, *Becn2*$^{flox/flox}$;TH-Cre mice showed less locomotion stimulation (Fig. 3A) and CPP (Fig. 3B) in response to cocaine than control mice, suggesting that Becn2 in DA neurons is important for cocaine-induced psychomotor stimulation and reward-learning behaviors.

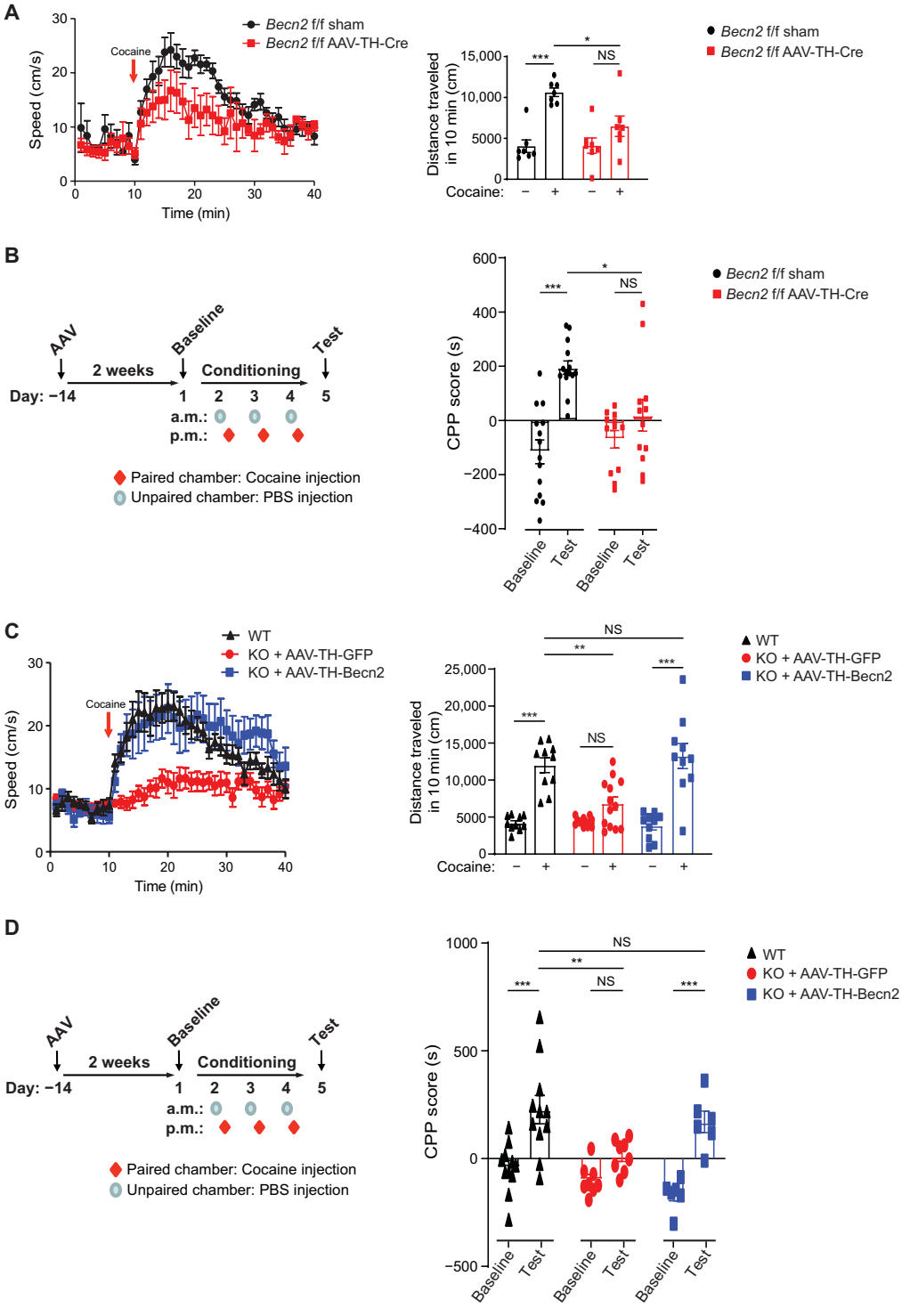

Fig. 3. Becn2 functions in DA neurons to regulate cocaine-induced locomotor activation and reward learning. (**A**) Cocaine-stimulated locomotion of *Becn2*$^{flox/flox}$ (*Becn2*$^{f/f}$) mice sham-treated or stereotaxically microinjected with AAV expressing Cre driven by the TH promoter was monitored by open-field test upon intraperitoneal injection of cocaine (15 mg/kg; arrow). Right: Quantification of distance traveled in 10 min before and after cocaine treatment. $N = 7$ per group. (**B**) CPP of *Becn2*$^{flox/flox}$ (*Becn2*$^{f/f}$) mice sham-treated or stereotaxically microinjected with AAV expressing TH-Cre. The mice received alternate cocaine and PBS injection for 3 days (conditioning), and their time spent in the paired (cocaine-injecting) chamber and the unpaired (PBS-injecting) chamber was recorded before (Baseline) and after conditioning (Test). *Becn2*$^{f/f}$ sham, $N = 14$; *Becn2*$^{f/f}$ AAV TH-Cre, $N = 12$. (**C**) Cocaine-induced locomotion monitored by open-field test in *Becn2*$^{+/-}$ KO (KO) mice stereotaxically microinjected with AAV expressing Becn2 or GFP driven by the TH promoter upon intraperitoneal injection of cocaine (15 mg/kg; arrow). Right: Quantification of distance traveled in 10 min before and after cocaine treatment. WT, $N = 10$; KO + AAV-TH-GFP, $N = 13$; KO + AAV-TH-Becn2, $N = 10$. (**D**) CPP of WT and *Becn2*$^{+/-}$ KO mice stereotaxically microinjected with AAV expressing TH-Becn2 or TH-GFP. WT, $N = 11$; KO + AAV-TH-GFP, $N = 8$; KO + AAV-TH-Becn2, $N = 6$. $^{*}P < 0.05$; $^{**}P < 0.01$; $^{***}P < 0.001$.

On the other hand, we found that DA neuron–specific re-expression of WT Becn2 in the global *Becn2*$^{+/-}$ KO mice rescues their cocaine-induced behaviors. We delivered WT Becn2 driven by the TH promoter to *Becn2*$^{+/-}$ KO mouse brain via AAV2/9 by stereotaxic injection into the VTA (fig. S5) and found that re-expressing WT Becn2 in DA neurons is sufficient to rescue both cocaine-stimulated locomotion (Fig. 3C) and cocaine-induced reward-seeking behaviors (Fig. 3D) in the *Becn2*$^{+/-}$ KO mice. Together, these data suggest that Becn2 regulates cocaine-induced behaviors in DA neurons, which is consistent with our finding on the role of Becn2 in DA release.

Becn2 depletion restores presynaptic D2R in the NAc and prevents lysosomal trafficking of endocytosed D2R

We next sought to investigate the mechanism by which Becn2 functions in DA neurons. We found that loss of Becn2 causes a partial, but not a complete, defect in basal autophagy, evidenced by reduced flux of green fluorescent protein (GFP)–LC3 (the autophagosome reporter) puncta in the whole cell, soma, and major neurites of cultured primary DA neurons isolated from *Becn2*$^{+/-}$ KO mice (fig. S6A); reduced flux of LC3-II (autophagosome membrane-associated lipidated LC3) and p62 (the autophagy cargo receptor) in SH-SY5Y neuroblasts transfected with *Becn2* short hairpin RNA (shRNA) (fig. S6B); and reduced flux of endogenous LC3 puncta in DA neurons in the VTA of *Becn2*$^{+/-}$ KO mouse brain in vivo (fig. S6C). In addition, different from proteasomal inhibition by MG132 (*N*-carbobenzyloxy-L-leucyl-L-leucyl-L-leucinal) or lysosomal inhibition by chloroquine, Becn2 depletion does not cause a proteostasis impairment in SH-SY5Y neuroblasts (fig. S7, A and B). In addition, primary DA neurons isolated from *Becn2*$^{+/-}$ KO mice do not show a defect in cell morphology or growth, compared with those from WT littermates (fig. S7, C and D). Similarly, in vivo, the density of DA neuron neurites in the NAc is comparable in WT mice and *Becn2*$^{+/-}$ KO mice by TH immunostaining (fig. S7E), suggesting no apparent degeneration or death of DA neurons in *Becn2*$^{+/-}$ KO mice.

To study how Becn2 regulates DA release and signaling, we analyzed the level of key receptors in DA signaling in the striatum. We found that haplodeletion of neither *Becn2* nor *Becn1* affects the level of D1R (DA receptor 1) or DAT in the striatum (fig. S8A). Instead, we previously found that the level of D2R showed a trend of an increase in the whole brain of *Becn2*$^{+/-}$ KO mice by Western blot analysis (*17*). Because D2R is expressed both presynaptically in dopaminergic neurons and postsynaptically in D2R-positive medium spiny neurons in the NAc, to determine whether Becn2 affects presynaptic D2R that negatively regulates DA release, we adapted a biochemical method to isolate crude synaptosomes and presynaptic membranes prepared from the NAc of the control *Becn2*$^{flox/flox}$ mice and *Becn2*$^{flox/flox}$ mice injected with AAV-TH-Cre (fig. S8B). We validated our purification method using Synaptophysin (SVP38) and DAT as presynaptic markers and PSD95, Homer1, GluR1, and NR1 as postsynaptic markers (fig. S8B). We found that D2R is higher on presynaptic membranes in the NAc of *Becn2*$^{flox/flox}$; TH-Cre mice than in control mice (Fig. 4A), suggesting that Becn2 down-regulates presynaptic D2R in DA neurons. In support of the data, the presynaptic D2R level is also higher in the NAc, but not the prefrontal cortex, of the global *Becn2*$^{+/-}$ KO mice than that of WT littermates (fig. S8C). Together, these data support the hypothesis that D2R is a degradation target of Becn2 in DA neurons.

Further, through a biotin protection degradation assay in human embryonic kidney (HEK) 293 cells stably expressing Flag-D2R (*32*), we found that shRNA knockdown of *Becn2* (fig. S8D) blocks D2R degradation through the endocytic trafficking pathway after agonist treatment (Fig. 4B), suggesting that Becn2 is required for agonist-induced endolysosomal degradation of D2R. To further demonstrate how Becn2 regulates D2R stability, we analyzed the role of Becn2 in the intracellular trafficking of D2R in response to agonists, by examining D2R colocalization with different organelle markers. In the absence of Becn2 following shRNA knockdown, we found that D2R can still be endocytosed, but internalized D2R is trapped in endosomal structures instead of being transported to lysosomes (Fig. 4C). We did not detect changes in the amount of endosomes (EEA1) or lysosomes (LAMP1) upon Becn2 depletion (fig. S8E), suggesting that Becn2 does not affect the level of endosomes or lysosomes per se; rather, it affects D2R trafficking through the endolysosomal pathway.

In addition, we found that in the NAc of *Becn2*$^{flox/flox}$; TH-Cre mice, while D2R in presynaptic membrane fractions increases (Fig. 4A), there is only a slight increase of D2R in the total PNS (postnucleus supernatant) fraction, and the level of D2R in the intracellular cytosolic S2 (supernatant fraction 2) fraction is decreased rather than increased (fig. S8F). These data suggest that Becn2 depletion in DA neurons ultimately increases the plasma membrane–localized D2R but not the cytoplasmic pool of D2R, which we propose is caused by enhanced recycling of D2R to the cell surface upon Becn2 loss. To test this hypothesis, we analyzed D2R recycling in cultured cells. We found that in Becn2-deficient cells, most of the endocytosed D2R is recycled back to the cell surface after agonist removal, detected by pulse-chase fluorescence imaging of antibody-labeled cell surface D2Rs (Fig. 4D), suggesting that Becn2 plays an essential role in the endolysosomal trafficking of D2R and prevents it from recycling back to the plasma membrane. Together, these data suggest that Becn2 plays a pivotal role in down-regulating the levels of D2R in presynaptic DA neurons projecting to the NAc, by promoting lysosomal trafficking of endocytosed D2R.

D2R antagonism rescues cocaine-induced behaviors and extracellular DA accumulation in *Becn2* KO mice

To further test the hypothesis that the effect of Becn2 depletion is mediated through D2R up-regulation, we determined whether D2R antagonists would rescue cocaine-induced behaviors in *Becn2*$^{+/-}$ KO mice to the WT level. Because it is reported that D2R antagonists preferentially inhibit presynaptic D2R autoreceptors when used at low doses (*33*, *34*), we injected the mice with vehicle or the highly selective D2R antagonist L-741,626 at a low dose (3 mg/kg) (*35*, *36*) 30 min before each cocaine injection in open-field and CPP experiments. Consistent with previously reported results (*37*), L-741,626 at the dose of 3 mg/kg does not increase cocaine-stimulated locomotion in WT mice; however, we found that L-741,626 treatment effectively rescued the peak of cocaine-stimulated locomotion in *Becn2*$^{+/-}$ KO mice to the WT level (Fig. 5A). We noticed that in global *Becn2* KO mice, D2R antagonist treatment rescued the peak level, but not the complete time course, of cocaine-induced locomotion (Fig. 5A). We reasoned that the partial rescue is possibly due to a relatively lower DA storage caused by increased D2R autoreceptor upon Becn2 depletion, leading to a faster DA depletion. In addition, L-741,626 also rescued the cocaine reward behavior in *Becn2*$^{+/-}$ KO mice to the WT level (Fig. 5B). Consistent with cocaine-induced behaviors, we found that L-741,626 treatment 30 min before cocaine injection also rescues cocaine-induced extracellular DA accumulation in the NAc of *Becn2*$^{+/-}$ KO mice to the WT level, by

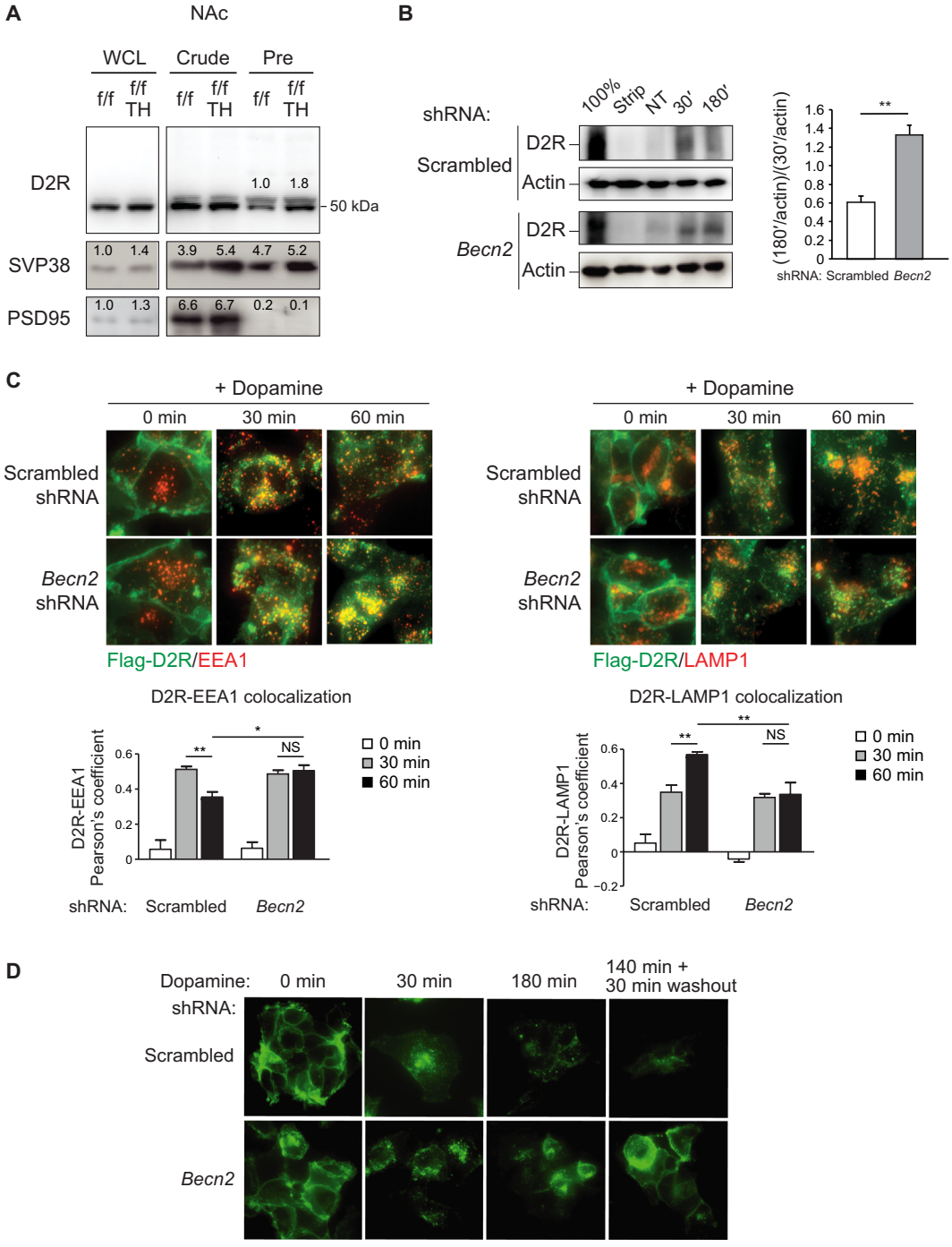

Fig. 4. Becn2 promotes D2R endolysosomal degradation and down-regulates presynaptic D2R on DA neurons. (**A**) Synaptosomes and the presynaptic membrane fraction were isolated from the NAc pooled from 10 *Becn2*$^{flox/flox}$ mice sham-treated or stereotaxically microinjected with AAV expressing TH-Cre. WCL, whole-cell lysates; Crude, crude synaptosomes; Pre, presynapses. Synaptophysin (SVP38), presynaptic marker; PSD95, postsynaptic marker. Quantification is shown above each protein band. f/f, *Becn2*$^{flox/flox}$; f/f TH, *Becn2*$^{flox/flox}$ TH-Cre. (**B**) Biotin protection degradation assay in HEK293 cells stably expressing Flag-D2R transfected with scrambled or *Becn2* shRNA. 100%, total biotinylated D2R; strip, remaining biotinylated D2R after cell surface stripping of biotin; NT, levels of internalized biotinylated D2R with vehicle treatment after stripping; "30'" and "180'", levels of internalized biotinylated D2R with agonist treatment (10 μM DA) for 30 or 180 min, respectively, after stripping. Biotinylated Flag-D2R was precipitated with anti-Flag antibody, analyzed by SDS-PAGE, and detected with streptavidin overlay. $N = 3$ independent experiments. (**C**) Immunofluorescence imaging on trafficking of endocytosed D2R to endosomes (EEA1) or lysosomes (LAMP1). Flag-D2R HEK293 cells transfected with scrambled or *Becn2* shRNA were fed with anti-Flag antibody and treated with the agonist DA for 30 or 60 min. Colocalization between D2R and EEA1 or LAMP1 was calculated as the Pearson's correlation coefficient. Data are shown as means ± SEM of three independent experiments ($N = 3$); in each experiment, a minimum of 60 cells under each condition were used for analyses. (**D**) Immunofluorescence imaging on Flag-D2R recycling. Flag-D2R HEK293 cells transfected with scrambled or *Becn2* shRNA were fed with anti-Flag antibody and treated with DA for 30 or 180 min or with DA for 140 min followed by agonist washout for 30 min. *$P < 0.05$; **$P < 0.01$.

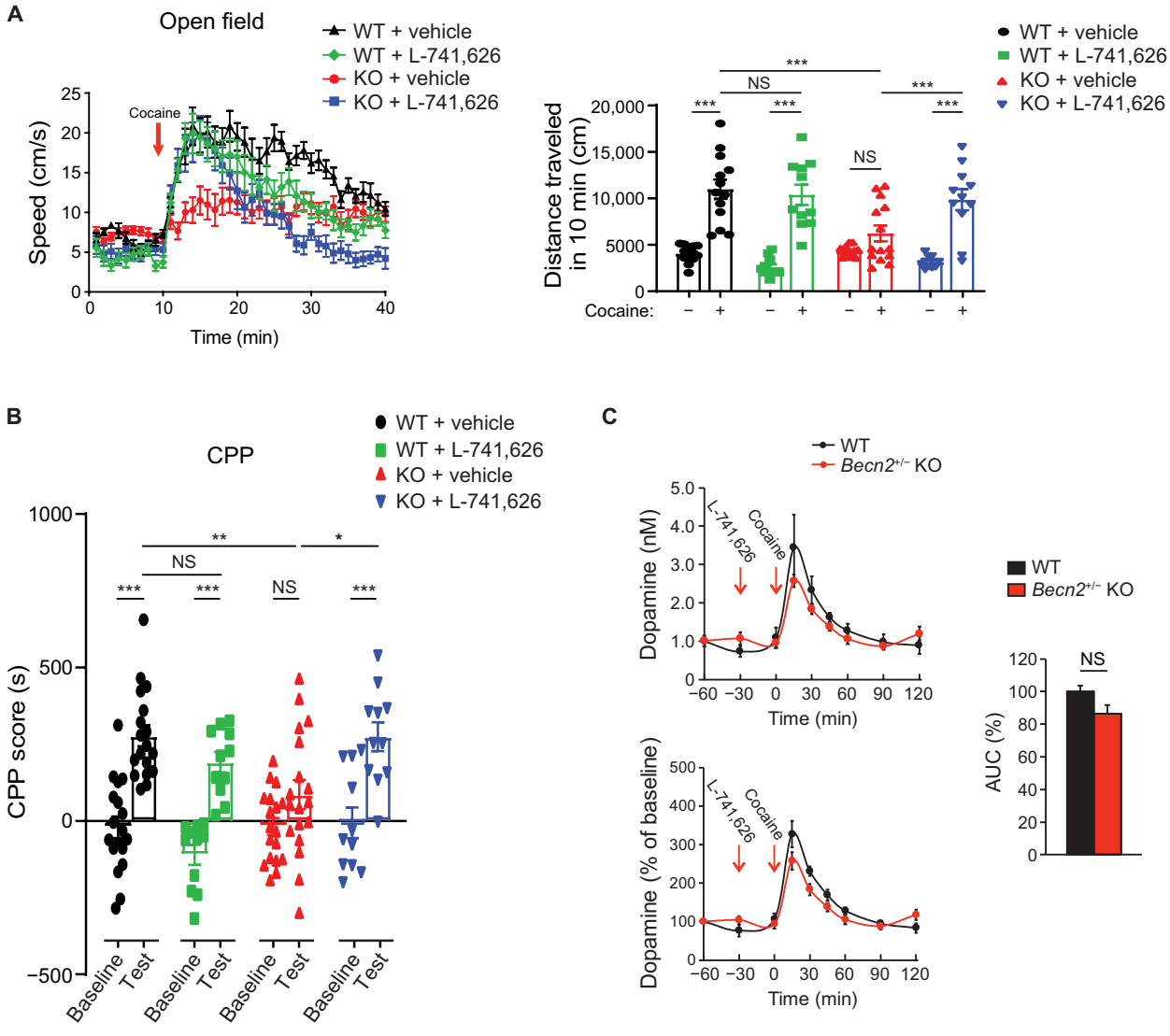

Fig. 5. D2R antagonism rescues cocaine-induced psychomotor stimulation, reward seeking, and DA accumulation in *Becn2*$^{+/-}$ KO mice. (**A**) Cocaine-stimulated locomotion of *Becn2*$^{+/-}$ KO mice is partially rescued by D2R antagonism. WT or *Becn2*$^{+/-}$ KO (KO) mice received injection of the selective D2R antagonist L-741,626 (3 mg/kg) 30 min before cocaine injection during open-field test. Open-field locomotion and quantification of distance traveled in 10 min before and after cocaine treatment are shown. WT + vehicle, $N = 13$; WT + L-741,626, $N = 11$; KO + vehicle, $N = 14$; KO + L-741,626, $N = 11$. (**B**) D2R antagonism rescues cocaine-induced CPP of *Becn2* KO mice. WT and *Becn2* KO mice were subjected to 3-day conditioning [alternate PBS injection in the morning (a.m.) and cocaine injection (15 mg/kg) in the afternoon (p.m.)]. During conditioning, mice were injected with vehicle or L-741,626 (3 mg/kg) 30 min before each cocaine injection. CPP scores at baseline and after conditioning were recorded. WT + vehicle, $N = 18$; WT + L-741,626, $N = 11$; KO + vehicle, $N = 18$; KO + L-741,626, $N = 11$. (**C**) Microdialysis analyses showing concentration and percentage of the baseline of DA in the NAc of *Becn2*$^{+/-}$ KO mice and WT littermates treated with L-741,626. Area under the curve is quantified for 120 min after cocaine injection. $N = 5$ mice per group. $^*P < 0.05$; $^{**}P < 0.01$; $^{***}P < 0.001$.

microdialysis/UPLC (Fig. 5C). Thus, we concluded that Becn2 regulates the behavioral effects of cocaine by down-regulating D2R in presynaptic DA neurons.

Becn2 regulates cocaine-induced physiological and behavioral responses by binding to D2R-associated GASP1

In the presence of agonists (such as DA), D2Rs are internalized and bind to GASP1 (GPCR-associated sorting protein 1) (*32*, *38*, *39*), which is required for the lysosomal degradation of D2R independently of ubiquitination or components of the canonical ESCRT (endosomal sorting complex required for transport) machinery (*40*, *41*). However, little is known regarding the molecular mechanisms of D2R down-regulation in response to cocaine in vivo. We previously found that GASP1 is a binding partner of Becn2 and identified a small region (amino acids 69 to 88) of human Becn2, as well as a single residue within this region (isoleucine at position 80; I^{80}), that mediates the interaction with GASP1 (*17*, *42*). To study the function of Becn2-GASP1 binding in D2R regulation, we expressed the loss-of-GASP1 interaction human Becn2 mutants, $Becn2^{\Delta 69\text{-}88}$ and $Becn2^{I80S}$, in HEK293 cells stably expressing Flag-D2R. Using biotin protection degradation assays, we found that both $Becn2^{\Delta 69\text{-}88}$ and $Becn2^{I80S}$

significantly delay DA-induced degradation of D2R (fig. S9A), suggesting that the Becn2-GASP1 interaction is required for D2R degradation. To study whether Becn2 regulates D2R degradation and cocaine-induced behaviors via GASP1 binding, we mapped the corresponding GASP1-binding residues in mouse Becn2 to amino acids 77 to 98 (homologous to human Becn2 amino acids 69 to 88) and the serine at position 97 within this region of mouse Becn2 (fig. S9B).

By coimmunoprecipitation analyses, we found that a deletion mutant of amino acids 91 to 98 Becn2$^{\Delta 91\text{-}98}$, as well as a point mutant Becn2^{S97L}, abolishes Becn2-GASP1 binding in mouse cell lines (Fig. 6A). To further analyze the mechanism of Becn2 in cocaine reward in vivo, we used the CRISPR-Cas9 technique (*43*) to generate a Becn2^{S97L} KI mouse model (fig. S9, C to E), in which we confirmed a loss of interaction between endogenous Becn2 and GASP1 in the brain by coimmunoprecipitation (Fig. 6B). The Becn2^{S97L} KI mice show normal viability, development, and fertility. Thus, we have identified a point mutation in mouse Becn2 that blocks its interaction with GASP1 and generated a new Becn2^{S97L} mouse model to study the function of Becn2-GASP1 interaction in cocaine-induced behavior and DA signaling. We found that similar to *Becn2*$^{+/-}$ KO mice, Becn2^{S97L} KI mice (losing GASP1 interaction) have significantly decreased locomotor activity stimulated by two different doses of cocaine (15 and 30 mg/kg) in open-field tests, compared to WT littermates (Fig. 6C and fig. S1A), suggesting that the Becn2-GASP1 interaction is essential for cocaine-stimulated behavior. Furthermore, we investigated whether removing Becn2-GASP1 interaction protects mice from the effects of repeated cocaine dosage. Repeated cocaine usage leads to behavioral sensitization to cocaine, as indicated by further enhancement of drug-induced locomotor stimulation (*9*, *44*). We found that after 8 days of repeated cocaine treatment, both *Becn2*$^{+/-}$ KO mice and loss-of-GASP1 interaction Becn2^{S97L} KI mice show reduced locomotion sensitization in open-field tests, compared to WT littermates (Fig. 6D), suggesting that the Becn2-GASP1 interaction, as well as Becn2, is essential for mediating the sensitizing effect of cocaine. Together, these data suggest that Becn2 plays an essential role in the regulation of the behavioral effects of cocaine via GASP1 binding, and blocking Becn2-GASP1 binding protects mice from these effects.

To support the conclusions, we further studied whether Becn2 regulates cocaine-induced striatal DA signaling via GASP1 binding. We measured cocaine-induced MEK and ERK phosphorylation in WT and Becn2^{S97L} KI mice with and without acute cocaine treatment. We found that cocaine induces phosphorylation of MEK and ERK in WT mice, but fails to do so in Becn2^{S97L} mice, in the NAc (Fig. 6E), suggesting that Becn2-GASP1 binding is required for cocaine-induced DA signaling. In addition, by synaptosome studies, we found that similar to Becn2 deletion, the Becn2^{S97L} mutant also increases the presynaptic D2R level in the NAc (Fig. 6F), suggesting that the interaction between Becn2 and GASP1 is crucial for presynaptic D2R degradation. In sum, these data support a model in which Becn2 regulates D2R degradation, cocaine-induced kinase signaling, and behavioral stimulation through interacting with the D2R adaptor GASP1 (Fig. 6G).

Autophagy inhibitors upstream of Becn2 prevent the behavioral effects of cocaine in WT mice

Our data suggest that Becn2 is a potential target for the prevention of cocaine-responsive behaviors. Since Becn2 is an autophagy-related protein and is regulated by upstream autophagy regulators, we propose that upstream autophagy inhibitors can inactivate Becn2 and prevent cocaine-induced DA signaling and behaviors. To test our hypothesis, we studied the therapeutic potential of two brain-penetrable small molecules that inhibit autophagy at early stages upstream of Becn2, SBI-0206965 and Spautin-1: SBI-0206965 inhibits the ULK1 kinase (*45*), which is an upstream kinase essential for activating the Vps34 PtdIns 3-kinase and autophagy (*46*, *47*), and Spautin-1 destabilizes the Vps34 kinase complex by inhibiting the deubiquitinating enzymes USP10 and USP13 (*48*). We found that compared to vehicle, treatment of WT mice with either SBI-0206965 or Spautin-1 for 5 days before a single dosage of cocaine significantly reduces cocaine-stimulated locomotion in open-field tests (Fig. 7A). Furthermore, we found that a 5-day treatment of SBI-0206965 (or Spautin-1) prevents acquisition of cocaine-induced reward learning in WT mice by CPP tests (Fig. 7B). Thus, we concluded that upstream autophagy inhibitors can reduce cocaine-induced locomotion and reward behaviors. Notably, SBI-0206965 or Spautin-1 does not lead to a further prevention of cocaine-induced locomotion (Fig. 7A) or CPP (Fig. 7B) in *Becn2*$^{+/-}$ KO mice, suggesting that the effect of the upstream autophagy inhibitors on cocaine-induced behaviors is through Becn2. Given these findings, as well as the aforementioned data demonstrating that the cocaine-stimulated behavior is specifically affected by Becn2 but not Becn1 (Fig. 1A), we propose that the effect of upstream autophagy inhibitors on cocaine responses is mediated through Becn2 but not bulk autophagy degradation.

Autophagy inhibition restores presynaptic D2R autoreceptor and prevents cocaine-induced extracellular DA accumulation and signaling

Cocaine acts by binding to the DAT, blocking the removal of DA from the synapse, and resulting in elevated extracellular DA levels. To determine whether autophagy inhibition upstream of Becn2 affects cocaine-induced DA accumulation, we measured DA levels after an acute cocaine injection in WT mice pretreated with the ULK1 kinase inhibitor SBI-0206965 for 8 days. We performed microdialysis in the NAc of freely moving mice, and the dialysates collected were quantified using the liquid chromatography–mass spectrometry (LC-MS) method (*49*). Consistent with the findings from *Becn2*$^{+/-}$ KO mice, we found that pretreatment of WT mice with SBI-0206965 significantly attenuated cocaine-induced DA accumulation in the NAc (Fig. 8A). In addition, in line with reduced DA accumulation, SBI-0206965 inhibits cocaine-induced kinase activation, including MEK and ERK, in the striatum of WT mice (Fig. 8B). These data support our model that inhibition of autophagy at early stages prevents cocaine-induced DA accumulation and signaling. Furthermore, via synaptosome studies, we found that similar to the effect of Becn2 depletion, treatment with the autophagy inhibitor SBI-0206965 increases the presynaptic level of D2R in both the striatum (Fig. 8C) and the NAc (fig. S10) of WT mice but does not further increase presynaptic D2R in *Becn2*$^{+/-}$ KO mice (fig. S10), suggesting that the effects of the upstream autophagy inhibitor on D2R metabolism is through Becn2. These findings support our model that Becn2-regulated D2R degradation can also be prevented by upstream autophagy inhibitors. In summary, these data support our model that upstream autophagy modulators regulate cocaine-induced DA signaling and behavioral responses (Fig. 8D): Autophagy inhibitors reduce DA signaling and prevent cocaine-responsive behaviors and have therapeutic potential against adverse effects of psychostimulant drugs.

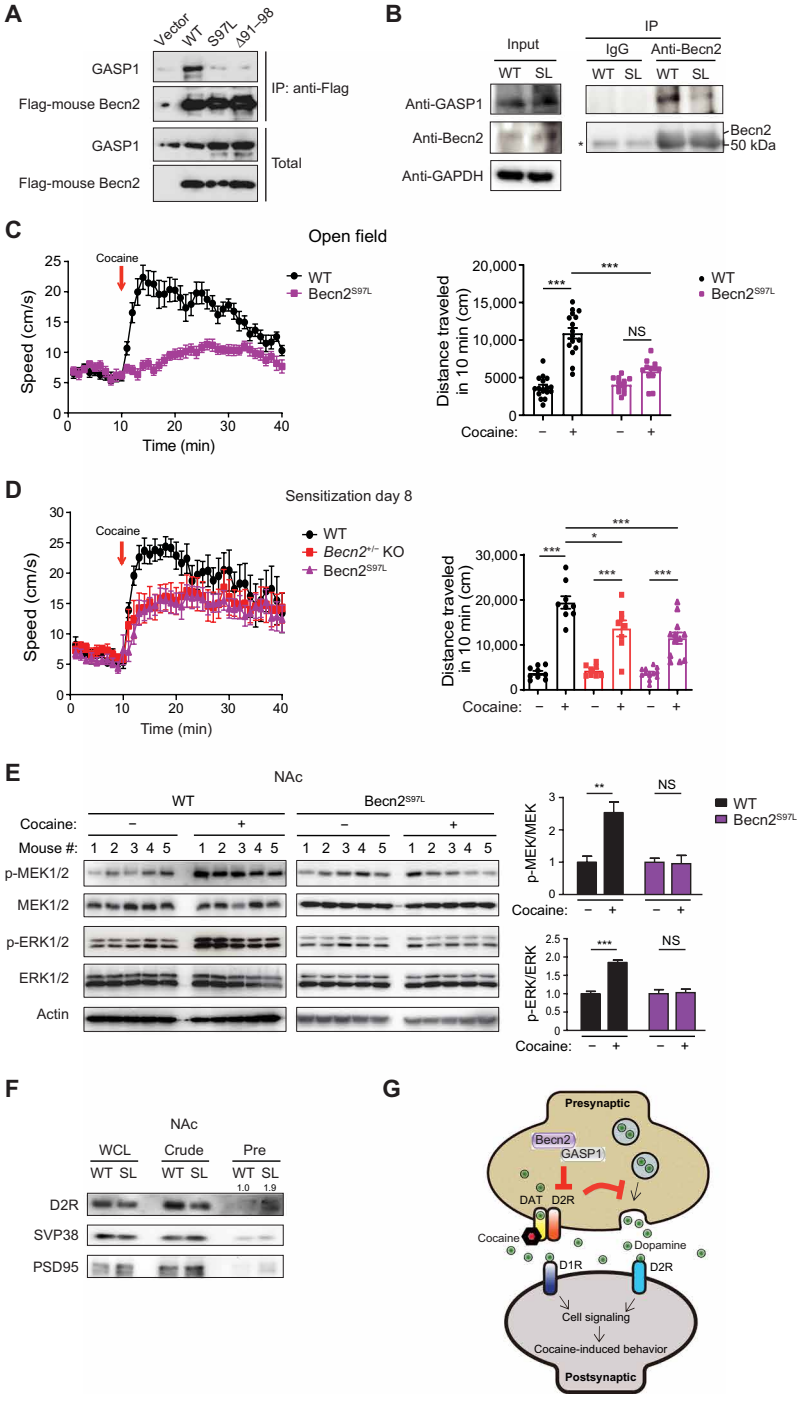

Fig. 6. Becn2 regulates the behavioral and physiological effects of cocaine by interacting with GASP1. (**A**) Identification of the mouse Becn2 S97L point mutation that abolishes Becn2-GASP1 binding in mouse cells. Coimmunoprecipitation of endogenous GASP1 in Neuro2A cells transfected with indicated Flag-tagged mouse Becn2 constructs. IP, immunoprecipitation. (**B**) Coimmunoprecipitation of GASP1 by Becn2 in brain lysates of WT and Becn2^{S97L} KI mice. SL, S97L; IgG, immunoglobulin G. (**C**) Left: Locomotor activity of WT and Becn2^{S97L} KI mice monitored by open-field test upon injection of cocaine (15 mg/kg). Right: Quantification of distance traveled in 10 min before and after cocaine treatment. WT, $N = 16$; Becn2^{S97L}, $N = 12$. (**D**) *Becn2*$^{+/-}$ KO and Becn2^{S97L} KI mice show reduced behavioral sensitization to repeated cocaine dosage, monitored by open-field test of WT, *Becn2*$^{+/-}$ KO, or Becn2^{S97L} mice after eight consecutive days of cocaine treatment. WT, $N = 9$; *Becn2*$^{+/-}$ KO, $N = 8$; Becn2^{S97L}, $N = 12$. (**E**) Western blot analyses of cocaine-induced MEK and ERK phosphorylation in the NAc of WT and Becn2^{S97L} KI mouse brain 15 min after cocaine or vehicle intraperitoneal injection. $N = 5$ mice. (**F**) The Becn2^{S97L} mutant increases presynaptic D2R in the NAc. Western blot analyses of D2R in whole-cell lysates, crude synaptosomes, and presynapses in the NAc pooled from 10 WT or Becn2^{S97L} mice. Synaptophysin (SVP38), presynaptic marker; PSD95, postsynaptic marker. Quantification is shown above each protein band. (**G**) Model of the autophagy protein Becn2 in the regulation of dopaminergic transmission and cocaine-induced behaviors. We propose that Becn2 mediates cocaine responsiveness (stimulation, sensitization, and reward) by down-regulating presynaptic D2Rs and promoting DA release via interacting with GASP1. Red D2R, presynaptic D2R; blue D2R, postsynaptic D2R; D1R, DA receptor 1. *$P < 0.05$; **$P < 0.01$; ***$P < 0.001$.

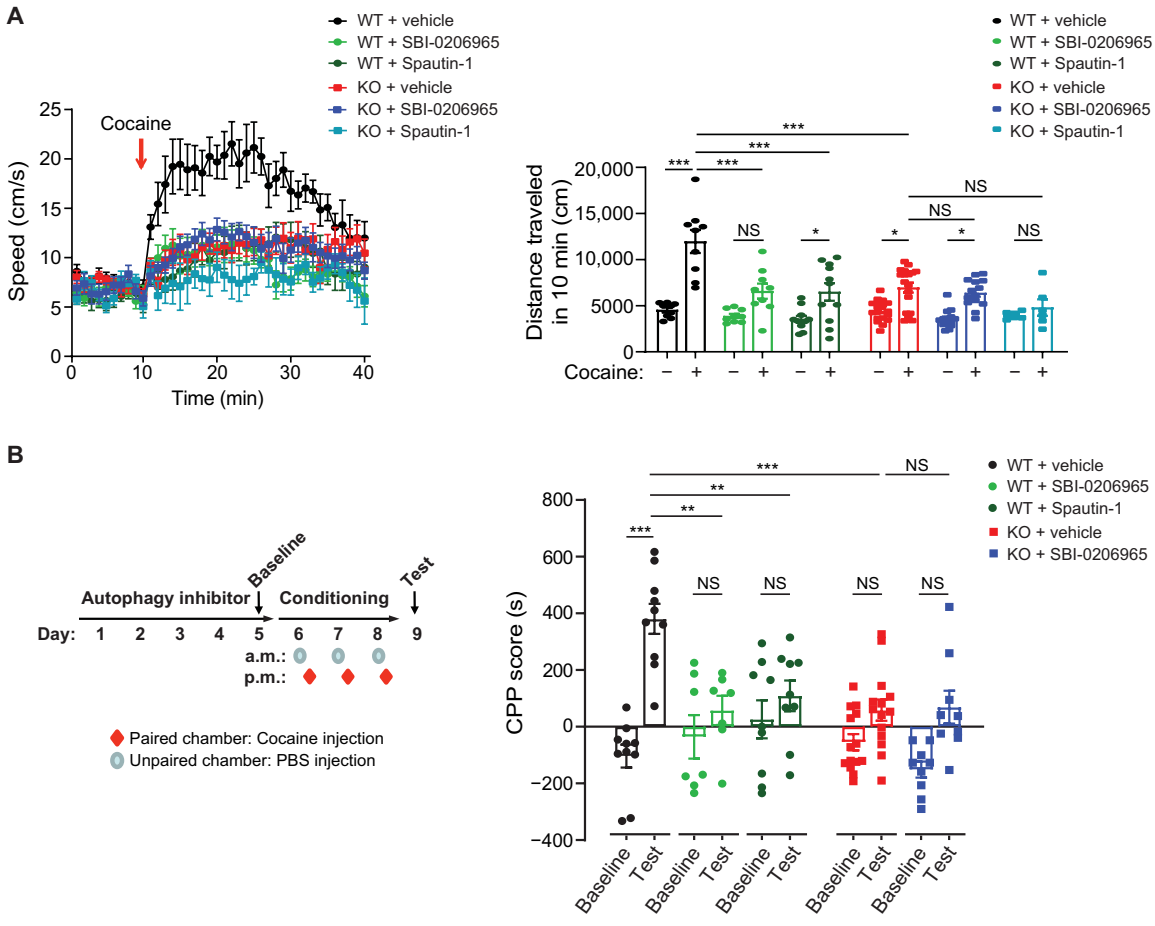

Fig. 7. Autophagy inhibitors upstream of Becn2 prevent cocaine-induced locomotion and reward learning. (**A**) A ULK1 kinase inhibitor and a Vps34 kinase complex inhibitor prevent locomotion stimulation by cocaine. Left: Cocaine-induced hyperactivity monitored by open-field test of WT and *Becn2*$^{+/-}$ KO (KO) mice intraperitoneally treated with vehicle or autophagy inhibitors (2 mg/kg) SBI-0206965 or Spautin-1 once daily for 5 days, before cocaine injection (15 mg/kg). Right: Distance traveled in 10 min before and after cocaine injection in open field by WT and *Becn2*$^{+/-}$ KO (KO) mice treated with vehicle, SBI-0206965, or Spautin-1. WT + vehicle, $N = 9$; WT + SBI-0206965, $N = 9$; WT + Spautin-1, $N = 11$; KO + vehicle, $N = 18$; KO + SBI-0206965, $N = 15$; KO + Spautin-1, $N = 6$. (**B**) Autophagy inhibition reduces CPP to repeated cocaine dosage. WT or *Becn2*$^{+/-}$ KO (KO) mice were treated with vehicle (DMSO) or autophagy inhibitors [SBI-0206965 (2 mg/kg) or Spautin-1 (2 mg/kg)] once daily for 5 days, followed by 3-day conditioning [alternate PBS injection in the morning (a.m.) and cocaine injection in the afternoon (p.m.)]. CPP scores at baseline and after conditioning were recorded. WT + vehicle, $N = 10$; WT + SBI-0206965, $N = 7$; WT + Spautin-1, $N = 9$; KO + vehicle, $N = 14$; KO + SBI-0206965, $N = 9$. $^*P < 0.05$; $^{**}P < 0.01$; $^{***}P < 0.001$.

DISCUSSION

Drug addiction is a chronic disease affecting reward, motivation, memory, and related circuitry in the brain. Drug abuse not only afflicts patient health and creates a burden on the health care system but also causes a variety of societal problems. DA is a key neurotransmitter that plays a pivotal role in drug addiction through its actions in the mesolimbic system. Increases in striatal DA have been implicated in the psychomotor-stimulating, behavioral-sensitizing, and addictive effects of cocaine. New ways of treating drug abuse involving novel drug targets are urgently needed. The data presented here highlight the haploinsufficiency of the autophagy gene *Becn2* in cocaine-induced behaviors (locomotor stimulation, behavioral sensitization, and reward) (Figs. 1 and 6D and fig. S1A), cocaine-amplified DA release (Fig. 2A and fig. S2C), and kinase signaling (Fig. 2, B and C, and fig. S2D), suggesting that Becn2 is required for cocaine-induced physiological and behavioral responses. Notably, we noticed that in *Becn2*$^{+/-}$ KO mice, baseline locomotion and DA levels (without cocaine) are similar to those in WT mice. We reason that under basal conditions, one copy of WT *Becn2* is sufficient to maintain a certain level of tonic DA release, and differences only become evident (amplified) in the presence of cocaine.

DA release is regulated by multiple neuronal populations, including DA neurons, GABAergic interneurons, and striatal cholinergic interneurons (*4*). By conditional KO of *Becn2* using *Becn2* floxed mice and rescue of Becn2 in global KO mice, we mapped the function of Becn2 in the development of cocaine reward primarily to DA neurons (Fig. 3). Nonetheless, although we propose that Becn2 in DA neurons plays a pivotal role in the regulation of cocaine responses, we cannot completely rule out that other neurons in the DA circuitry also facilitate Becn2-regulated cocaine-induced behaviors by indirectly regulating DA neuron firing or function (e.g., compare cocaine-stimulated locomotion in Fig. 3A to Fig. 1A). In the AAV-directed rescue experiment, although the majority (86%) of GFP-expressing cells are TH-positive DA neurons, we detected that 14% of GFP-expressing cells did not show the TH signal, suggesting a leakage of expression from the AAV-rTH-PI-GFP construct in a small population

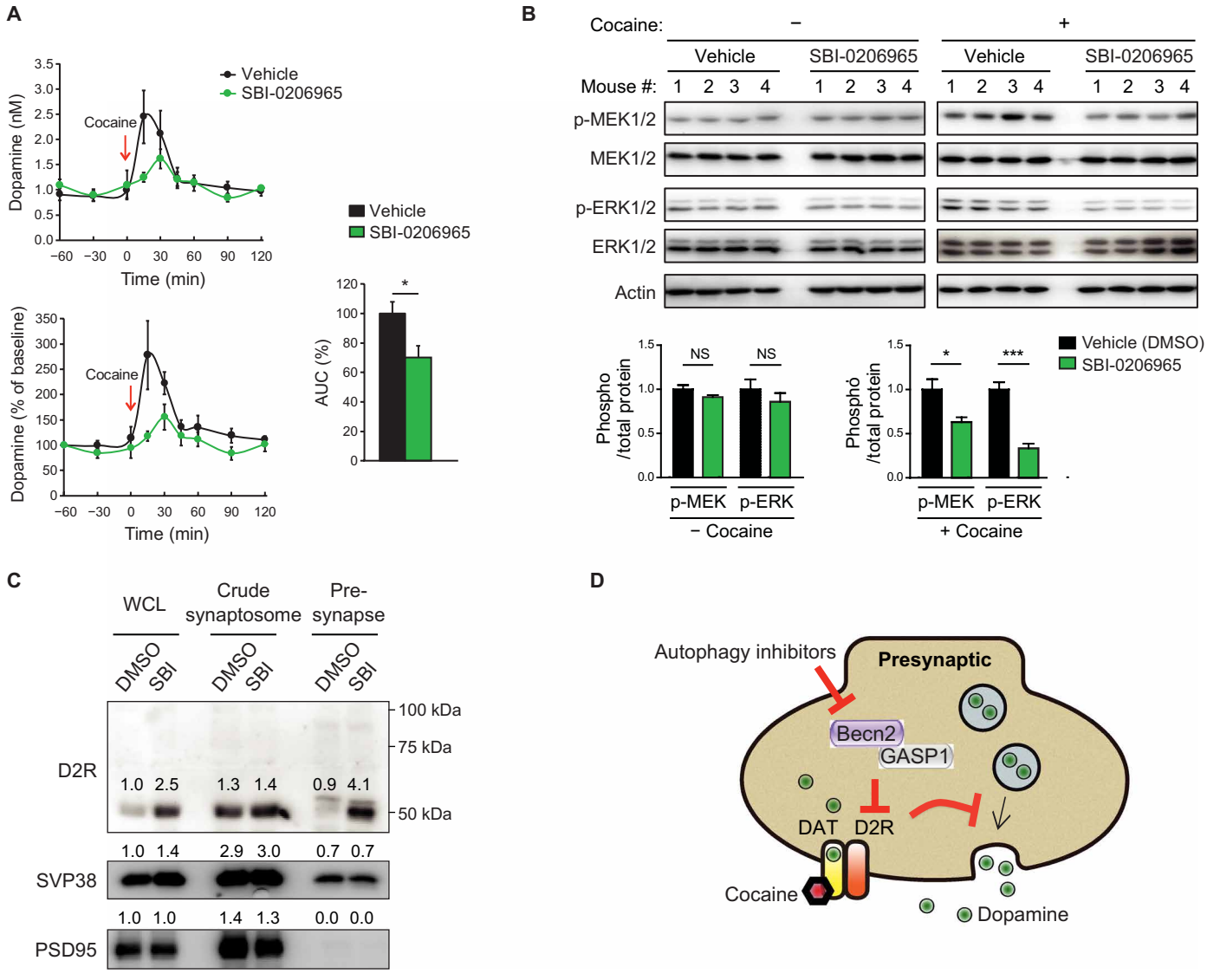

Fig. 8. Autophagy inhibition upstream of Becn2 restores striatal presynaptic D2R and prevents cocaine-amplified DA release and signaling. (**A**) Microdialysis analyses showing concentration and percentage of the baseline of DA in the NAc of WT mice pretreated with SBI-0206965 or vehicle. Area under the curve is quantified for 120 min after cocaine injection. $N = 6$ mice per group. (**B**) Striatal tissues were collected 15 min after intraperitoneal injection of cocaine or vehicle from WT mice treated with vehicle or SBI-0206965 (2 mg/kg) once daily for 5 days. Western blot analyses of cocaine-induced MEK and ERK phosphorylation are shown. $N = 4$ mice. (**C**) The upstream autophagy inhibitor SBI-0206965 increases presynaptic D2R in the striatum. Western blot analyses of D2R in whole-cell lysates, crude synaptosomes, and presynapses in the striatum pooled from eight WT mice intraperitoneally treated with either vehicle (DMSO) or SBI-0206965 (SBI) at 2 mg/kg once daily for 5 days. Synaptophysin (SVP38), presynaptic marker; PSD95, postsynaptic marker. Quantification is shown above each protein band. (**D**) Model on how upstream autophagy inhibitors prevent cocaine-induced dopaminergic transmission and behavioral responses via Becn2. The function of the Becn2-GASP1 complex on D2R autoreceptor degradation and DA release is prevented by autophagy inhibitors upstream of Becn2. $^{*}P < 0.05$; $^{***}P < 0.001$.

of non-DA neurons in the VTA. Whether Becn2 plays a role in other types of neuronal cells in the VTA region is worthy of investigation in the future. The use of other neuronal Cre lines (such as ChAT-Cre and VGAT-Cre mice) will be helpful to comprehensively understand the role of Becn2 in the DA system.

Our data also suggest that presynaptic D2R in the NAc is a critical degradation target of Becn2. Mutant mice that lack D2 receptors self-administered cocaine at higher rates than their heterozygous or WT littermates, and pretreatment with the D2-like antagonist increased rates of self-administration of cocaine (*50*). This is consistent with our finding that global or DA neuron–specific depletion of Becn2 increases presynaptic D2R autoreceptor levels (Fig. 4A and fig. S8C) and decreases cocaine reward behaviors (CPP and IVSA; Figs. 1 and 3).

By imaging, we found that in the absence of Becn2, D2R is recycled back to the plasma membrane instead of being degraded in lysosomes (Fig. 4). Thus, we propose a model that down-regulating D2R autoreceptors is the underlying mechanism of Becn2 in DA release and cocaine responses (Fig. 6G). In this model, we propose that the effect of Becn2 on D2R degradation is not through general endosomal

or autophagic degradation of membrane receptors, because we found that on one hand, Becn2 does not affect the level of other important DA signaling molecules either in presynaptic neurons (such as DAT) or in postsynaptic neurons (such as D1R) (fig. S8A), as well as other molecules including the chemokine receptor CXCR4 and the receptor tyrosine kinase platelet-derived growth factor receptor (*17*); on the other hand, another autophagy protein Becn1 does not affect cocaine-induced behavior (Fig. 1A).

Mechanistically, we found that the binding between Becn2 and the D2R-associated protein GASP1 is key for D2R degradation and behavioral stimulation in response to cocaine. Becn2 point mutant mice lacking GASP1 binding (Becn2^{S97L} KI) are protected from hyperactivity and kinase signaling stimulated by cocaine as are *Becn2*$^{+/-}$ KO mice (Fig. 6, C to E). Consistent with the prevention of cocaine-induced behaviors in *Becn2*$^{+/-}$ KO mice and Becn2^{S97L} KI mice, GASP1 KO mice have also been reported to show attenuated hyperlocomotion and behavioral sensitization to cocaine (*51*, *52*), further supporting our model that GASP1 is the adaptor protein linking D2R to Becn2 for down-regulation and mediating the function of Becn2 in cocaine responses. Our sequence analysis on Becn2 and GASP1 also explains the previous observation that there is a species specificity with respect to Becn2-GASP1 interactions; i.e., human GASP1 only interacts with human, but not mouse, Becn2, and vice versa (*17*). The protein alignment revealed that mutating I^{80} to serine (S) in human Becn2 blocks its binding with human GASP1; notably, mouse Becn2 contains a threonine (T), which is structurally and biochemically similar to serine, at the same residue position (fig. S9B). Likewise, in mouse Becn2, if S97 is substituted by L (the corresponding residue in human Becn2), the Becn2-GASP1 binding is also abolished (Fig. 6, A and B).

Although besides D2R autoreceptors, we have not identified other receptors regulated by Becn2 that might also be associated with reduced DA release thus far, we cannot completely rule this out. In the future, proteomic approaches might be used to systemically profile Becn2-regulated cell surface receptors, for example, TMT (tandem mass tag) labeling followed by MS in whole brain and different brain regions (including NAc, VTA, and prefrontal cortex) of WT and Becn2 mutant mice (including *Becn2*$^{+/-}$ KO and Becn2^{S97L} KI mice). These studies will help address whether there are key candidate receptors other than D2R that may also show an increase in both *Becn2*$^{+/-}$ KO and Becn2^{S97L} KI mice.

Together, we propose that Becn2 promotes DA release from the axon terminal by degrading D2R autoreceptors via GASP1 binding, thereby enhancing the stimulating and addictive effects of cocaine (Fig. 6G). The model raises the possibility that targeting Becn2 may be a new strategy in treating the effects of many abusive drugs whose actions involve DA release in the limbic system. We therefore proposed that upstream autophagy inhibitors that block the function of Becn2 would suppress cocaine-induced DA accumulation, DA signaling, and behavior. This idea is supported by our data that a number of autophagy inhibitors (including SBI-0206965 and Spautin-1) that block early-stage autophagy kinases inhibit cocaine-induced locomotor stimulation and reward behaviors, kinase activation, and DA release (Figs. 7 and 8). SBI-0206965 or Spautin-1 does not show further prevention of cocaine-induced locomotion (Fig. 7A) or CPP (Fig. 7B) in *Becn2*$^{+/-}$ KO mice, demonstrating that the effect of these inhibitors on cocaine-induced behaviors is through Becn2. In addition, SBI-0206965 does not further increase presynaptic D2R levels in *Becn2*$^{+/-}$ KO mice (fig. S10), suggesting that the effects of the upstream autophagy inhibitor on D2R metabolism is also through Becn2. Hence, our research provides the first evidence suggesting that the autophagy protein Becn2 is a previously unknown potential therapeutic target for treating cocaine-induced disorders. Note that during drug treatment for cocaine responses, we avoided long-term autophagy inhibition, because we reasoned that chronically blocking a degradation pathway might affect proteostasis and cause potential side effects in vivo. Instead, the protocol we used was short-term autophagy inhibitor treatment (5 days) (Figs. 7 and 8). We have tested the safety of the autophagy-inhibiting compounds (including SBI-0206965 and Spautin-1) administered by intraperitoneal injection for 4 weeks at the indicated dose and did not detect obvious adverse effects on mouse survival or activity. However, to fully rule out that short-term autophagy inhibitor usage may have side effects, various metabolic parameters will have to be closely monitored in mice, for example, through the use of metabolic cages.

In summary, these studies demonstrate how an autophagy-related gene regulates psychostimulant-evoked physiological and behavioral responsiveness via the DA circuitry. Future studies will be helpful to demonstrate the in-depth mechanisms of Becn2 and its autophagy binding partners in cocaine seeking and relapse including electrophysiology, signal transduction, and gene expression, as well as elucidating related neuronal circuits. To achieve such goals, we have generated useful genetic tools, including global and conditional *Becn2* KO mice, as well as the KI mouse line loss of binding with GASP1, to further understand the mechanism and physiological link among Becn2, autophagy, and drug responsiveness. We propose that in addition to cocaine responses, Becn2 and autophagy-modulating compounds may regulate a variety of mental disorders and drug abuse syndromes that involve DA signaling, such as depression, schizophrenia, and addiction to other drugs of abuse such as amphetamine and methamphetamine.

MATERIALS AND METHODS

Animals

All animal experiments have been approved by the Northwestern University Institutional Animal Care and Use Committee. All mice were maintained on a 14-hour light/10-hour dark cycle at an ambient temperature of 22°C and 42% humidity. All mice used in the study were male adult mice in the C57BL/6J background. The global *Becn1*$^{+/-}$ and *Becn2*$^{+/-}$ heterozygous KO mice have been described previously (*17*, *27*). DAT-Cre mice were obtained from the Jackson Laboratory (JAX #006660).

Behavioral experiments were conducted during the light cycle. Male mice at 8 to 12 weeks of age were used for behavioral testing and were acclimated to the test room at least 1 hour before the initiation of all experiments. Cocaine (Sigma-Aldrich, C5776) was dissolved in PBS.

Conditional *Becn2*$^{flox/flox}$ mice were generated using a targeting vector in which exon1 and exon2 of *Becn2* were flanked by LoxP sites, and a neomycin cassette flanked by FRT sites was inserted between exon2 and the 3′ LoxP site (fig. S4A). Ten micrograms of targeting vector was linearized and electroporated into C57BL/6 × 129/SvEv hybrid embryonic stem (ES) cells. After selection with G418, surviving clones were expanded for polymerase chain reaction (PCR) analysis to identify recombinant ES clones, using the forward primer 5′-TGTGTCAGTTTCATAGCCTGAAGAACGAG-3′ and reverse primer 5′-GGCATAGCCTCATTTCCTTCCTGGG-3′.

Secondary confirmation of positive clones identified by PCR was performed by Southern blotting analysis, using the probes indicated in fig. S4A. Briefly, genomic DNA was digested with Sac I or Nco I and electrophoretically separated on 0.8% agarose gel. After transfer to a nylon cellulose membrane, the digested DNA was hybridized with the probe targeted against the 5′ external region after Sac I digestion: CTGCCCAAAGCTGGAAAGTGGAAAGAGACATAGTACACCTGACATCATGAGAAGAGAATAATAATACTCCCTGGAATGAGATAGTCACTAAACTACCTGAGAAGCCTTCCTTCAGCACAGGTGGGTGCCTGTGGATCCTCACTGCTCGGCTGCACTTACCAGGCAATGTGTTTCTCTCCTTCTTCGCCTCCTCCTTCTCCAATACCTGTCTCCTTTCTCAGACACTCACTCATTTCTATTTTCTCTCTGGACCCAGGCTGGCCTTCCTCTGGAGTCCCAGGTCCCACCACAGCTGGCAACAGTTTCTAAGCACCATTGAGTCTAGTCGAACACTGCCTGATTGTCCATGCTGCGCTCTAAGATAGCTTGTACTTCATTCACTTCCAAACAAAGAAGCTGAACATCGAGTTCATAAATAAACTGTTAGTGAAACGAAATTAGCACCACAGGCTCTCTGCATCCAAATATTGTATCATATCAGGAGCAGCGAAAGATTGGCTA, and with the probe targeted against the 3′ internal region after Nco I digestion: ACGGAGACAGGCACATGACACAAAAGCTTGCTCTAGCTCTTTCCATCATAGGCTCTGAGCCATATTCAACAATGGTTACTTTTGCTTTATGTTTTGAGGTTCGTAGAAAGGAACGATGCCAAGCCCAACAGAAGGTCTCAAGCCATCACACAATCACCAGCCAAGGAAGTTTTGACGTGAGAGGAAGCTCCAACAGTGAGGGTCGTTGAGACAAAACTTCCTCAACTCAGATCCTTGTAGTCACAGTATGACAGCACAATGTTAGAAGCTGGGATCCCAGGAAAAGCAGGGAAGTTGGGGAAAGTTGGCCTCGAGAGGATCAGACAGAGCTGGCCACAGACAGTTATGAGGGTGTGAAGAACTCCAGTCTGCTCATTGAGTTCAGAGTCATATCGTGGACAATAGTCACTGGATCAGAGAATAGCAGCAAGATGTGTCTGGACAAG. Offspring were genotyped for the floxed allele by PCR with the forward primer CCCGGCTTAGACTTTTTTCTAAAGATG and the reverse primer GAGGTAAGCAGAGTAAAAGTGCAGAG. The *Becn2*$^{flox/flox}$ mice were backcrossed to the C57BL/6J strain for >10 generations.

Becn2^{S97L} KI mice were generated by the CRISPR-Cas9 strategy. Briefly, the targeting construct containing a Neomycin cassette flanked by LoxP sites and the TCT→TTG mutation was electroporated into C57BL/6 ES cells. G418-resistant clones were picked, screened by PCR with the forward primer GCTGACCGCTTCCTCGTGCTTTA and the reverse primer GAATGGAATGTCTCTTGAGTTCGCAG, and sequenced by the sequencing primer TGGCCGTCTAAATCCTCTAGCTCC. Secondary confirmation of positive ES clones identified by PCR was performed by Southern blot analyses, using a probe targeting the Neomycin cassette (Neo-probe) amplified by the Neo-probe forward primer TCATCTCACCTTGCTCCTGC and the Neo-probe reverse primer AAGGCGATAGAAGGCGATGC. ES clones containing the KI allele showed a 6.6-kb band after Eco RV digestion and a 9.0-kb band after Hind III digestion. Tertiary confirmation is performed by DNA sequencing using the sequencing primer 5′-TGATCCATTTCCAAATACGCTGC-3′.

Autophagy modulation

Autophagy inhibitors SBI-0206965 (APExBio, A8715) and Spautin-1 (AdooQ Bioscience, A12942) were dissolved in 100% dimethyl sulfoxide (DMSO) at stock concentrations of 20 mg/ml (SBI-0206965) and 25 mg/ml (Spautin-1), respectively. The stock solutions were then diluted in PBS to make a 0.2 mg/ml working concentration. Mice were intraperitoneally injected with vehicle (PBS), SBI-0206965, or Spautin-1 at 2 mg/kg of body weight once per day for 5 days before cocaine injection (15 mg/kg).

Open field

Locomotor activity was recorded using the LimeLight software (Coulbourn Instruments). Mice were habituated to the open-field arena (dimensions, 56 cm by 56 cm) for 20 min before intraperitoneal cocaine injection at different doses (5, 15, or 30 mg/kg). Activity was recorded for 30 min after cocaine administration. Comparison was performed between the distance traveled 10 min before cocaine injection (baseline) and the distance traveled during the interval of 5 to 15 min after cocaine injection. To measure behavioral sensitization to cocaine, mice were intraperitoneally injected with cocaine (15 mg/kg) once per day for 8 days, and locomotor was recorded on day 8 as described above.

Conditioned place preference

A randomized unbiased procedure was used. The chambers were rectangular in shape (45 cm by 20 cm by 20 cm) and consisted of two compartments with differences in visual and tactile cues, separated by a removable door. One compartment had walls with a black-and-white striped pattern, and the other had walls with black dots at a white background. The floors were interchangeable and consisted of distinct apertured or smooth textures. Overviews of the experimental setup and schedule are shown in Figs. 1B, 3, B and D, and 7B. The procedure consisted of three phases: baseline pretesting, conditioning, and the CPP test. Pretesting (baseline) took place on day 1, when the mice were given free access to the entire apparatus for a 20-min period, and the time spent in each of the two compartments was recorded and analyzed using the LimeLight software (Coulbourn Instruments).

For cocaine CPP, mice were administered with alternate intraperitoneal injections of cocaine (15 mg/kg) or PBS and then were placed into one conditioning chamber for PBS pairing and the other for cocaine pairing for 30 min after each injection. For food-induced CPP, mice were reduced to 85% of their ad lib weight over 7 days before the beginning of conditioning. Mice were maintained at this weight throughout the experiment and received their daily feeding 1 hour after conditioning sessions to eliminate mnemonic effects of chow. During the 50-min conditioning period, mice were given Froot Loops (food) in one chamber and nothing in the other chamber. The conditioning phase consisted of a 4-day schedule of double-conditioning sessions per day separated by an interval of at least 3 hours. Food was introduced on the baseline pretest day to habituate the mice to Froot Loops.

After conditioning, CPP testing (test) was conducted using the same procedure as in the pretest phase. A CPP score was calculated by subtracting the time spent in the PBS/no food–paired chamber from the time spent in the cocaine/food-paired chamber (seconds).

Jugular vein catheterization surgery and mouse self-administration

Mouse jugular vein catheterization surgery and mouse self-administration are adapted from our previous publication (*53*). Indwelling catheters were constructed of polyurethane tubing (inner diameter, 0.012″; outer diameter, 0.025″; Braintree Scientific Inc., Braintree, MA).

Becn2$^{+/-}$ and WT mice were anesthetized with isoflurane. Incisions were made on the skin of the head and ventral neck, and the right jugular vein was externalized. The end of the catheter was inserted into the jugular vein via a small incision and was secured to the vein and surrounding tissues with silk sutures (SouthPointe Surgical Supply Inc., Coral Springs, FL). The exit port of the catheter passed subcutaneously to the back where it was attached to a vascular access button (Instech, Plymouth Meeting, PA), which was embedded under mouse back skin and secured with suture. Buprenorphine (Sigma-Aldrich, St. Louis, MO) was subcutaneously administered (0.10 mg/kg) for postoperative analgesia once a day for at least 3 days. To extend catheter patency, the catheters were flushed once a day immediately after surgery or cocaine self-administration training with 0.05 ml of heparin in saline (30 U/ml; Thermo Fisher Scientific, Pittsburgh, PA). Cocaine IVSA was conducted in standard mouse operant conditioning chambers (ENV-307A, Med Associates, Georgia, VT) located in a behavioral procedure room. The chambers were equipped with nose-poke sensors (ENV-313M, Med Associates) in two holes located on one side of the chamber 1.0 cm above the floor; cue and hole lamps located, respectively, above and in each hole; and a house light located on the top of the chamber opposite the holes. During cocaine IVSA training, one hole was set as active and the other inactive. Nose pokes in the active hole triggered pump (PHM-100, Med Associates) infusions (3 s) and turned on both cue lamp and hole lamp (10 s). Nose pokes in the inactive hole and active hole during the timeout period (30 s) had no programmed consequences but were recorded. The vascular access button was connected to the spring tether (Instech, Plymouth Meeting, PA) via a magnetic adaptor for drug infusions. Swivels were suspended above the chamber. An infusion pump and a syringe were located inside of each cubicle.

After 3 to 7 days of recovery from the catheterization surgery, mice were initially subjected to 3-hour daily sessions of cocaine IVSA under a fixed ratio 1 (FR1) schedule for 5 days, and the cocaine reinforcement schedule was then changed to an FR2 for an additional 5 days. The unit dose of cocaine was used at 0.6 mg/kg per infusion over 3 s (infusion volume, 6.6 μl) for IVSA in our study. Stable IVSA, defined as deviations of less than 20% of the mean active responses in three consecutive training sessions, is established after 10 days of training. Following acquisition of IVSA, mice were tested for IVSA with unit doses of 0.1, 0.6, and 1 mg/kg per infusion of cocaine, respectively. Active and inactive responses to different doses were recorded for 3 hours for each dose.

Elevated zero maze

The level of anxiety of animals was assessed in the elevated zero maze test according to the method previously described (*54*). The zero maze apparatus consisted of a 5-cm-wide circular track with an inside diameter of 45 cm and elevation of 35 cm. It contained two open quadrants and two close quadrants enclosed by 15-cm-high walls. Mice were placed in one of the closed quadrants and allowed to investigate the zero maze for 5 min. During this time, the mice were traced to determine total distance, distance traveled in open quadrants, time spent in open quadrants, number of crossings, and latency by the LimeLight software (Coulbourn Instruments).

In vivo microdialysis and DA measurement

The in vivo microdialysis and DA measurement methods are adapted from previous literature (*55*). Adult mice weighing 25 to 30 g were used for intracerebral microdialysis. A guide cannula was stereotaxically implanted above mouse NAc [anterior-posterior (AP), +1.2 mm; medial-lateral (ML), ±1.0 mm; dorsal-ventral (DV), 4 mm] from bregma. Twenty-four hours after implantation, a microdialysis probe (2 mm dialyzing membrane, CMA-7, Harvard Apparatus, Cambridge, MA) was inserted into the guide cannula and lowered down to the NAc region in freely moving animals. The microdialysis probe was flushed with artificial cerebrospinal fluid at a flow rate of 1 μl/min using a microsyringe pump (Harvard Apparatus, Cambridge, MA). Once the probe was positioned, the probe was flushed at 1 μl/min for 180 min. Dialysate samples were collected at 60 and 30 min before and 0, 15, 30, 45, 60, 90, and 120 min after cocaine injection (15 mg/kg, ip). Ten microliters of dialysate was derivatized using BzCl. DA-1,1,2,2-d4 was used as an internal standard. At the completion of the experiment, animals were euthanized, and probe placement was confirmed with histology.

Derivatized dialysate samples were analyzed by LC-MS using Agilent 1290 UHPLC coupled to a 6460 triple quadrupole mass spectrometer (Santa Clara, CA) in multiple reaction monitoring mode. Five microliters of samples was injected onto an InfinityLab Porshell 120EC-C18 (2.1 mm × 100 mm, 4 μm, 100 Å pore size). Samples were analyzed in triplicate. Electrospray ionization was used in positive mode. Automated peak integration was performed using Agilent MassHunter Workstation Quantitative Analysis for QQQ; all peaks were visually inspected to ensure proper integration.

Synaptosome isolation

Purified synaptosomes were prepared through a discontinuous Percoll gradient as previously described (*56*, *57*) with modifications to obtain presynaptic membrane. A workflow of synaptosome isolation is displayed in fig. S8B. Briefly, mouse NAc and striatum were collected and homogenized with 10 volumes of ice-cold homogenizing buffer [320 mM sucrose, 1 mM EDTA, 0.3 mM dithiothreitol (DTT), and 5 mM tris (pH 7.4)] using Teflon-glass homogenizer with 12 strokes and centrifuged at 1000*g* for 10 min at 4°C (whole-cell lysate). The supernatant was further centrifuged at 17,000*g* for 20 min at 4°C, and the obtained pellet (crude synaptosomes) was resuspended in 300 μl of homogenizing buffer and 1.2 ml of 3% Percoll solution [3% Percoll, 320 mM sucrose,1 mM EDTA, 0.3 mM DTT, and 5 mM tris (pH 7.4)]. A Percoll gradient was made by layering 1.5 ml of 23% Percoll solution followed by 1.5 ml of 10% Percoll. Resuspended crude synaptosomes were deposited on top of the Percoll gradient and centrifuged at 31,000*g* for 5 min at 4°C. Centrifugation speed was decelerated from the maximum down to 500 rpm and then from 500 to 0 rpm. The synaptosome fraction was collected between the 10% and the 23% Percoll bands and washed in 10 volumes of sucrose/EDTA buffer [320 mM sucrose, 1 mM EDTA, and 5 mM tris (pH 7.4)] by centrifugation at 200,000*g* for 15 min at 4°C. The pellet was resuspended in 0.5% Triton X-100/2 mM EDTA solution, rotated for 15 min at 4°C, and centrifuged at 20,000*g* for 20 min at 4°C. The supernatant was used as the presynaptic membrane fraction, and the pellet was dissolved in 0.5% SDS/50 mM Hepes/2 mM EDTA solution as the postsynaptic density fraction.

Preparation of AAVs

The AAV-rTH-PI-Cre-SV40 plasmid and virus [1×10^{13} genomic copies (GC)/ml] were purchased from Addgene (no. 107788). AAV-rTH-PI-EGFP and AAV-rTH-PI-mBecn2 virus (7×10^{12} GC/ml) were generated by the Boston Children's Hospital Viral Core. The

AAV-rTH-PI-GFP and AAV-rTH-PI-mBecn2 plasmids were modified as follows. To construct the TH promoter–driving EGFP- and mBecn2-AAV plasmids, the pAAV-rTH-PI-Cre-SV40 (Addgene, no. 107788) was modified by replacement of the original Cre gene with the *EGFP* gene or *mBecn2* gene via the restriction sites Bsr GI and Xba I using the In-Fusion HD Cloning Kit (Takara). The resulting plasmids were named "pAAV-rTH-PI-EGFP" and "pAAV-rTH-PI-mBecn2 AAV." *EGFP* and *mBecn2* were cloned from the pEGFP-N1 (Takara) and Flag-CMV-mBecn2 plasmids (*17*), respectively, using the following primers: primers for AAV-rTH-PI-GFP construction: forward primer: 5′-AGTCGAGAATTGTACAGCCACCATGGTGAGCAAGGGCGAGGAGCTGTT-3′; reverse primer: 5′-GCGGCCCGACTCTAGACTACTTGTACAGCTCGTCCATGCCGAGAGA-3′; primers for AAV-rTH-PI-mBecn2 construction: forward primer: 5′-AGTCGAGAATTGTACAGCCACCATGTCTCCTGCCCTCTTCCT-3′; reverse primer: 5′-GCGGCCCGACTCTAGACTATTAAGGCCTCTGGACTCTGGAAAAC-3′.

Stereotaxic surgery

For intracranial injection, 7-week-old mice were deeply anesthetized by intraperitoneal injection of ketamine (100 mg/kg)/xylazine (10 mg/kg), placed in the stereotaxic apparatus (Stoelting Instruments), and intracranially injected with AAV-rTH-PI-Cre-SV40 (500 nl, 1.9×10^{13} viral genomes/ml), AAV-rTH-PI-EGFP (1 μl, 7×10^{12} GC/ml), or AAV-rTH-PI-mBecn2 AAV (1 μl, 9×10^{12} GC/ml) at 100 nl/min into the VTA (coordinates relative to bregma: AP, −3.2 mm; ML, 0.3 mm; DV, −4.3 mm). The injection tip was left in place for at least an additional 5 min and then slowly retracted. The incision was closed with sutures. Mice remained on a heating pad until fully recovered from anesthesia and were given meloxicam (0.2 mg/kg, subcutaneously) at 24-hour intervals for 2 days after surgery to aid recovery. Animals were allowed to recover and housed for 3 weeks to enable optimal virus expression before behavioral experiments.

Immunostaining of brain sections

Immunostaining of brain sections was used to validate AAV-directed gene targeting or expression (mice were euthanized 2 to 3 weeks after AAV administration) and to image DA neuron neurite density in the NAc. Brain tissues were collected after perfusion with PBS and 4% paraformaldehyde (PFA). PFA-fixed brain tissues were cryostat-sectioned at 40 μm thickness. Sections were permeabilized with 0.5% Triton X-100 for 30 min and then blocked in 5% normal goat serum for 1 hour at room temperature. Free-floating coronal sections were immunostained with anti-Becn2 (Millipore, ABC253), anti-GFP (Invitrogen, A11120), and anti-TH (Millipore, AB152 and MAB318) antibodies and then with Alexa Fluor or Alexa Fluor Plus 488–conjugated secondary antibody (Invitrogen, A-11008, A-11001, and A32723) and Alexa Fluor 594–conjugated secondary antibody (Invitrogen, A-11012 and A-11005). Slides were mounted using ProLong Diamond Antifade Mountant (Invitrogen, P36961). Fluorescence images were acquired using a Nikon CSU-W1 spinning disk confocal microscope. The images were analyzed using Nikon's NIS-Elements.

Rescue experiment with D2R antagonist

The D2R antagonist L-741,626 (AdooQ Bioscience, A133694) was dissolved in DMSO at the stock concentration of 30 mg/ml and then diluted in PBS to a working concentration of 0.3 mg/ml. Mice were intraperitoneally injected with vehicle (PBS) or L-741,626 at 3 mg/kg of body weight 30 min before cocaine injection (15 mg/kg) in an open-field test for locomotion analysis or at the conditioning phase of CPP.

Biotin protection degradation assay

The biotin protection degradation assay was performed essentially as previously described (*17*). HEK293 cells stably expressing Flag-tagged D2R were transfected with scrambled shRNA or *hBecn2* shRNA. After 72 hours, cells were washed with ice-cold PBS and incubated with Sulfo-NHS-SS-Biotin (0.3 mg/ml; Thermo Fisher Scientific, #21331) for 30 min at 4°C. After PBS wash, cells were then returned to warm media for treatment. Cells labeled with "100%" and "stripped" were left on ice in PBS. Other cells were treated with 10 μM DA for the indicated time (30 or 180 min) while "NT" was treated with DMSO as a vehicle control. Cells except the 100% group were then washed with cold PBS followed by treatment with the stripping solution (50 mM glutathione, 0.3 M NaCl, 75 mM NaOH, and 10% fetal bovine serum) at 4°C for 30 min. Cells were then treated with the quench solution (50 mM iodoacetamide and 1% bovine serum albumin in PBS) at 4°C for 20 min and extracted in lysis buffer [0.1% Triton X-100, 150 mM NaCl, 25 mM KCl, 1× proteinase inhibitor, and 10 mM tris (pH 7.4)]. The D2R receptor was immunoprecipitated using anti-Flag M2 antibody (Sigma-Aldrich) and Protein A/G PLUS-Agarose beads (Santa Cruz Biotechnology, sc-2003) at 4°C overnight. Precipitates were washed and treated with peptide *N*-glycosidase F (New England Biolabs, P0705) at 37°C for 2 hours, then denatured in SDS sample buffer without reducing agents, and separated by SDS–polyacrylamide gel electrophoresis (PAGE). Biotinylated proteins were visualized using the VECTASTAIN Elite ABC immunoperoxidase reagent (Vector Laboratories, PK6100). β-Actin from total cell lysates was used as an internal control for input.

Receptor trafficking and recycling assay by antibody pulse chase

The antibody-feeding immunofluorescence-recycling assay was performed as previously described (*42*, *58*). Briefly, HEK293 cells stably expressing Flag-D2R were transfected with scrambled shRNA or *hBecn2* shRNA. After 24 hours, cells were seeded on 0.5% gelatin-coated coverslips, grown for 48 hours, and then fed with anti-FLAG M1 antibody (Sigma-Aldrich, F3040) at the concentration of 3.5 μg/ml for 30 min. Cells were left untreated as "0 min" control or treated with the agonist (DA, 10 μM) for 30 or 60 min, and then washed with PBS without calcium to strip off the residual noninternalized M1 antibody (M1 interaction to Flag is calcium sensitive). Cells were fixed in 2% PFA (Sigma-Aldrich, P6148), permeabilized with 0.5% Triton X-100, and immunostained with anti-EEA1 (Invitrogen, MA5-14794) or anti-LAMP1 (Cell Signaling Technology, #9091) antibodies. An Alexa Fluor 488–conjugated secondary antibody (Invitrogen, A-11037) was used to detect Flag, and an Alexa Fluor 594–conjugated secondary antibody (Invitrogen, A11037) was used to detect EEA1 and LAMP1. Quantification of colocalization was done using the ImageJ "coloc2" plugin with Costes threshold regression. The level of colocalization between D2R and EEA1 or LAMP1 was calculated as Pearson's correlation coefficient, a well-established measure of linear correlation between two variables (fluorophores) in fluorescence microscopy (*59*).

To assess D2R recycling, cells were either fixed directly as 0-min control or treated with 10 μM DA for 30 or 180 min. Then, cells were washed in PBS without calcium to strip off noninternalized

M1 antibody. To assess recycled D2R ("140 + 30 min washout"), cells were subjected to agonist washout in PBS for 30 min, following agonist (10 μM DA) treatment for 140 min and M1 antibody strip-off. Cells were then fixed, permeabilized, and immunostained as described above.

Autophagy analysis

For measuring the GFP-LC3 flux by microscopy, GFP-LC3 homozygous transgenic mice were crossed to *hBecn2* heterozygous KO mice to generate GFP-LC3–expressing *Becn2*$^{+/-}$ KO mice. Primary DA neurons were isolated and cultured as previously described (*60*). Cells were treated with or without 100 nM bafilomycin A1 for 4 hours on day 10 in vitro. Cells were then fixed with 4% PFA, blocked, and immunostained with anti-TH primary antibody (Millipore, AB152) and Alexa Fluor 594–conjugated secondary antibody (Invitrogen, A-11012). GFP-LC3 puncta were quantified by fluorescence microscopy.

For measuring the LC3 and p62 flux by Western blot analysis, SH-SY5Y cells were transfected with pLKO.1-scrambled shRNA or pLKO-*hBecn2* shRNA (targeting site: AATTGGACTGCAGTTTCAGAG, NM_001290693.1,906-926). Seventy-two hours after transfection, cells were treated with or without 100 nM bafilomycin A1 for 4 hours. Cells were washed with DPBS and lysed in radioimmunoprecipitation assay (RIPA) buffer, and lysates were analyzed by Western blot analysis. The intensity of the LC3 and p62 bands was determined by the ImageJ software.

For measuring the LC3 flux in vivo, mice were intraperitoneally injected with PBS or chloroquine (50 mg/kg). Four hours following the injection, brain tissues were collected after perfusion with PBS and 4% PFA. PFA-fixed brain tissues were cryostat-sectioned at 40 μm thickness. Sections were permeabilized with 0.5% Triton X-100 for 30 min and then blocked in 5% normal goat serum for 1 hour at room temperature. Free-floating coronal sections were immunostained with anti-TH (Millipore, MAB318) and anti-LC3 (Cell Signaling Technology, 3868) antibodies and then with Alexa Fluor Plus 488–conjugated secondary antibody (Invitrogen, A32723) and Alexa Fluor Plus 594–conjugated secondary antibody (Invitrogen, A32740). Slides were mounted using ProLong Diamond Antifade Mountant (Invitrogen, P36961), and fluorescence images were acquired using a Nikon CSU-W1 spinning disk confocal microscope. The number of LC3 puncta (autophagosomes) was counted using the ImageJ software.

Proteostasis assay

Protein proteostasis and aggregation were assessed using the PROTEOSTAT Protein Aggregation Assay (ENZO, ENZ-51023). Proteostat is a molecular rotor dye that specifically detects protein aggregates, inclusion bodies, and aggresome-like structures in cells and cell lysates. SH-SY5Y cells were transfected with pLKO.1-scrambled shRNA or pLKO-*Becn2* shRNA (targeting site: AATTGGACTGCAGTTTCAGAG, NM_001290693.1,906-926). Seventy-two hours after transfection, scrambled shRNA–transfected cells were treated with or without 10 μM proteasomal inhibitor MG132 for 4 hours or 50 μM lysosomal inhibitor chloroquine for 16 hours. Cells were then stained with Proteostat according to the manufacturer's instructions and observed by fluorescence microscopy. For quantification of Proteostat fluorescence, 3 μg of protein was loaded in black-bottom 96-well microplates, and the Proteostat detection dye was added. Samples were incubated in the dark for 15 min. Fluorescence intensity values were collected on a BioTek Synergy HT microplate reader.

Reverse transcription PCR

Total RNA was isolated from the prefrontal cortex and the VTA using the TRIzol reagent (Invitrogen) and treated with DNA-free reagent (Invitrogen, AM1906). One microgram of total RNA was used for complementary DNA (cDNA) synthesis using the High-Capacity cDNA Reverse Transcription Kit (Applied Biosystems, 4368814). Reverse transcription PCR was performed using the Platinum Taq DNA Polymerase (Invitrogen). The primers used were as follows: *Becn2* forward primer: GACTGTCTTCAGCAGTTTGTGG; *Becn2* reverse primer: GTCAGCACTCAGGGGTCTAAG; *Cre* recombinase forward primer: CGACCAGGTTCGTTCACTCA; *Cre* recombinase reverse primer: CAGCGTTTTCGTTCTGCCAA; *36B4* forward primer: TTCGTGTTCACCAAGGAGGAC; *36B4* reverse primer: ATGATCAGCCCGAAGGAGAAG.

Coimmunoprecipitation

For analysis of mouse Becn2-GASP1 interaction in vitro, mouse Neuro2A cells were transfected with Flag-tagged mouse Becn2 constructs. At 48 hours after transfection, cells were lysed with lysis buffer [50 mM tris (pH 8.0), 150 mM NaCl, 1 mM EDTA, 10% glycerol, 1% Triton X-100, and protease inhibitor cocktail]. To assess mouse Becn2-GASP1 interaction in vivo, mouse brain was homogenized in the above lysis buffer using the Dounce homogenizer. The lysates were centrifuged at 14,000 rpm at 4°C for 20 min. The supernatant was incubated with M2 anti-Flag antibody (Sigma-Aldrich) for cells or with Becn2 antibody (Novus) for mouse brain and Protein A/G PLUS-Agarose beads (Santa Cruz Biotechnology, sc-2003) with constant agitation at 4°C for 2 hours. The precipitates were washed three times with wash buffer [20 mM tris (pH 8.0), 150 mM NaCl, 1 mM EDTA, and 0.1% Triton X-100] and denatured in SDS loading buffer at 95°C for 5 min. Eluates were separated by SDS-PAGE and analyzed by Western blot analysis.

Western blot analysis

Cell or mouse brain protein was extracted in RIPA lysis buffer containing 50 mM tris (pH 7.4), 150 mM NaCl, 1 mM EDTA, 1% Triton X-100, and halt protease and phosphatase inhibitor cocktail (Thermo Fisher Scientific, 78440) and subjected to Western blot analysis. For analysis of kinase phosphorylation, NAc and striatal tissues were isolated from mouse brain 15 min after cocaine (15 mg/kg) or vehicle intraperitoneal injection. The following antibodies were used in Western blot analysis: anti-MEK1/2 (Cell Signaling Technology, 9122), anti–phospho-MEK1/2 Ser^{217}/Ser^{221} (Cell Signaling Technology, 9121), anti-p42/44 MAPK (ERK1/2) (Cell Signaling Technology, 9102), anti–phospho-p42/44 MAPK (ERK1/2) Thr^{202}/Tyr^{204} (Cell Signaling Technology, 9101), anti-CREB (Cell Signaling Technology, 9197), anti–phospho-CREB Ser^{133} (Cell Signaling Technology, 9198), anti-GASP1 (anti-GPRASP1, Prestige Antibodies, Sigma-Aldrich, HPA000161), anti-Becn1 (Santa Cruz Biotechnology, sc-11427), anti-Becn2 (Novus, NB110-60984 and NB110-60982), anti–Flag-HRP (horseradish peroxidase) (Sigma-Aldrich, A8592), anti-D1R (Sigma-Aldrich, D2944), anti-DAT (Millipore, MAB369), anti-D2R (Abcam, ab85367), anti-Synaptophysin (SVP38, Abcam, ab8049), anti-PSD95 (Novus, NB-300-556), anti-Homer1 (Antibodies-online Inc., ABIN1742339), anti-GluR1 (AMPA-R1, Millipore, AB1504), anti-NR1 (NMDA-R1, Abcam, ab109182), anti-Synapsin1/SYN1 (Cell Signaling Technology, 5297), anti-LC3 (Novus, NB100-2220), anti-p62 (BD Biosciences, 610833), and anti-ACTB/β-actin–HRP (Santa Cruz Biotechnology, sc47778

HRP) antibodies. Band intensity of Western blot gel lanes was quantified by the ImageJ software.

Statistical analysis

Statistical analysis was performed using the indicated analysis of variance (ANOVA) or Student's *t* test methods with the Excel or GraphPad Prism software (table S1). The data shown are the means ± SEM. *P* values less than 0.05 were considered a significant difference.

SUPPLEMENTARY MATERIALS

Supplementary material for this article is available at http://advances.sciencemag.org/cgi/content/full/7/8/eabc8310/DC1

View/request a protocol for this paper from *Bio-protocol*.

REFERENCES AND NOTES

1. W. J. Lynch, K. L. Nicholson, M. E. Dance, R. W. Morgan, P. L. Foley, Animal models of substance abuse and addiction: Implications for science, animal welfare, and society. *Comp. Med.* **60**, 177–188 (2010).
2. M. P. Saddoris, J. A. Sugam, F. Cacciapaglia, R. M. Carelli, Rapid dopamine dynamics in the accumbens core and shell: Learning and action. *Front. Biosci. (Elite Ed.)* **5**, 273–288 (2013).
3. C. Lüscher, The emergence of a circuit model for addiction. *Annu. Rev. Neurosci.* **39**, 257–276 (2016).
4. D. Sulzer, How addictive drugs disrupt presynaptic dopamine neurotransmission. *Neuron* **69**, 628–649 (2011).
5. N. D. Volkow, J. S. Fowler, G. J. Wang, R. Baler, F. Telang, Imaging dopamine's role in drug abuse and addiction. *Neuropharmacology* **56** (suppl. 1), 3–8 (2009).
6. Y. Schmitz, C. Schmauss, D. Sulzer, Altered dopamine release and uptake kinetics in mice lacking D_2 receptors. *J. Neurosci.* **22**, 8002–8009 (2002).
7. M. Benoit-Marand, E. Borrelli, F. Gonon, Inhibition of dopamine release via presynaptic D2 receptors: Time course and functional characteristics *in vivo*. *J. Neurosci.* **21**, 9134–9141 (2001).
8. F. Rougé-Pont, A. Usiello, M. Benoit-Marand, F. Gonon, P. V. Piazza, E. Borrelli, Changes in extracellular dopamine induced by morphine and cocaine: Crucial control by D2 receptors. *J. Neurosci.* **22**, 3293–3301 (2002).
9. A. L. Chausmer, J. L. Katz, The role of D_2-like dopamine receptors in the locomotor stimulant effects of cocaine in mice. *Psychopharmacology* **155**, 69–77 (2001).
10. M. Welter, D. Vallone, T. A. Samad, H. Meziane, A. Usiello, E. Borrelli, Absence of dopamine D2 receptors unmasks an inhibitory control over the brain circuitries activated by cocaine. *Proc. Natl. Acad. Sci. U.S.A.* **104**, 6840–6845 (2007).
11. E. P. Bello, Y. Mateo, D. M. Gelman, D. Noaín, J. H. Shin, M. J. Low, V. A. Alvarez, D. M. Lovinger, M. Rubinstein, Cocaine supersensitivity and enhanced motivation for reward in mice lacking dopamine D_2 autoreceptors. *Nat. Neurosci.* **14**, 1033–1038 (2011).
12. B. J. Everitt, D. Belin, D. Economidou, Y. Pelloux, J. W. Dalley, T. W. Robbins, Review. Neural mechanisms underlying the vulnerability to develop compulsive drug-seeking habits and addiction. *Philos. Trans. R. Soc. Lond. B Biol. Sci.* **363**, 3125–3135 (2008).
13. P. K. Thanos, N. D. Volkow, P. Freimuth, H. Umegaki, H. Ikari, G. Roth, D. K. Ingram, R. Hitzemann, Overexpression of dopamine D2 receptors reduces alcohol self-administration. *J. Neurochem.* **78**, 1094–1103 (2001).
14. P. Gorwood, Y. Le Strat, N. Ramoz, C. Dubertret, J.-M. Moalic, M. Simonneau, Genetics of dopamine receptors and drug addiction. *Hum. Genet.* **131**, 803–822 (2012).
15. N. D. Volkow, M. Morales, The brain on drugs: From reward to addiction. *Cell* **162**, 712–725 (2015).
16. D. Martinez, A. Broft, R. W. Foltin, M. Slifstein, D.-R. Hwang, Y. Huang, A. Perez, W. G. Frankel, T. Cooper, H. D. Kleber, M. W. Fischman, M. Laruelle, Cocaine dependence and D_2 receptor availability in the functional subdivisions of the striatum: Relationship with cocaine-seeking behavior. *Neuropsychopharmacology* **29**, 1190–1202 (2004).
17. C. He, Y. Wei, K. Sun, B. Li, X. Dong, Z. Zou, Y. Liu, L. N. Kinch, S. Khan, S. Sinha, R. J. Xavier, N. V. Grishin, G. Xiao, E.-L. Eskelinen, P. E. Scherer, J. L. Whistler, B. Levine, Beclin 2 functions in autophagy, degradation of G protein-coupled receptors, and metabolism. *Cell* **154**, 1085–1099 (2013).
18. W. Zhang, C. He, Regulation of plasma membrane receptors by a new autophagy-related BECN/Beclin family member. *Autophagy* **10**, 1472–1473 (2014).
19. N. Mizushima, A. Yamamoto, M. Matsui, T. Yoshimori, Y. Ohsumi, In vivo analysis of autophagy in response to nutrient starvation using transgenic mice expressing a fluorescent autophagosome marker. *Mol. Biol. Cell* **15**, 1101–1111 (2004).
20. A. Rocchi, C. He, Regulation of exercise-induced autophagy in skeletal muscle. *Curr. Pathobiol. Rep.* **5**, 177–186 (2017).
21. N. Mizushima, M. Komatsu, Autophagy: Renovation of cells and tissues. *Cell* **147**, 728–741 (2011).
22. A. Rocchi, S. Yamamoto, T. Ting, Y. Fan, K. Sadleir, Y. Wang, W. Zhang, S. Huang, B. Levine, R. Vassar, C. He, A *Becn1* mutation mediates hyperactive autophagic sequestration of amyloid oligomers and improved cognition in Alzheimer's disease. *PLOS Genet.* **13**, e1006962 (2017).
23. S. Yamamoto, K. Kuramoto, N. Wang, X. Situ, M. Priyadarshini, W. Zhang, J. Cordoba-Chacon, B. T. Layden, C. He, Autophagy differentially regulates insulin production and insulin sensitivity. *Cell Rep.* **23**, 3286–3299 (2018).
24. L. Cao, M. P. Walker, N. K. Vaidya, M. Fu, S. Kumar, A. Kumar, Cocaine-mediated autophagy in astrocytes involves sigma 1 Receptor, PI3K, mTOR, Atg5/7, beclin-1 and induces type II programed cell death. *Mol. Neurobiol.* **53**, 4417–4430 (2016).
25. P. Guha, M. M. Harraz, S. H. Snyder, Cocaine elicits autophagic cytotoxicity via a nitric oxide-GAPDH signaling cascade. *Proc. Natl. Acad. Sci. U.S.A.* **113**, 1417–1422 (2016).
26. D. Hernandez, C. A. Torres, W. Setlik, C. Cebrián, E. V. Mosharov, G. Tang, H.-C. Cheng, N. Kholodilov, O. Yarygina, R. E. Burke, M. Gershon, D. Sulzer, Regulation of presynaptic neurotransmission by macroautophagy. *Neuron* **74**, 277–284 (2012).
27. X. Qu, J. Yu, G. Bhagat, N. Furuya, H. Hibshoosh, A. Troxel, J. Rosen, E.-L. Eskelinen, N. Mizushima, Y. Ohsumi, G. Cattoretti, B. Levine, Promotion of tumorigenesis by heterozygous disruption of the beclin 1 autophagy gene. *J. Clin. Invest.* **112**, 1809–1820 (2003).
28. C. P. O'Brien, E. L. Gardner, Critical assessment of how to study addiction and its treatment: Human and non-human animal models. *Pharmacol. Ther.* **108**, 18–58 (2005).
29. J.-M. Beaulieu, R. R. Gainetdinov, The physiology, signaling, and pharmacology of dopamine receptors. *Pharmacol. Rev.* **63**, 182–217 (2011).
30. K. Brami-Cherrier, E. Valjent, D. Hervé, J. Darragh, J.-C. Corvol, C. Pages, A. J. Simon, J.-A. Girault, J. Caboche, Parsing molecular and behavioral effects of cocaine in mitogen- and stress-activated protein kinase-1-deficient mice. *J. Neurosci.* **25**, 11444–11454 (2005).
31. J. Chao, E. J. Nestler, Molecular neurobiology of drug addiction. *Annu. Rev. Med.* **55**, 113–132 (2004).
32. S. E. Bartlett, J. Enquist, F. W. Hopf, J. H. Lee, F. Gladher, V. Kharazia, M. Waldhoer, W. S. Mailliard, R. Armstrong, A. Bonci, J. L. Whistler, Dopamine responsiveness is regulated by targeted sorting of D2 receptors. *Proc. Natl. Acad. Sci. U.S.A.* **102**, 11521–11526 (2005).
33. S. W. Castro, P. G. Strange, Differences in the ligand binding properties of the short and long versions of the D2 dopamine receptor. *J. Neurochem.* **60**, 372–375 (1993).
34. A. Malmberg, D. M. Jackson, A. Eriksson, N. Mohell, Unique binding characteristics of antipsychotic agents interacting with human dopamine D2A, D2B, and D3 receptors. *Mol. Pharmacol.* **43**, 749–754 (1993).
35. B. J. Bowery, Z. Razzaque, F. Emms, S. Patel, S. Freedman, L. Bristow, J. Kulagowski, G. R. Seabrook, Antagonism of the effects of (+)-PD 128907 on midbrain dopamine neurones in rat brain slices by a selective D_2 receptor antagonist L-741,626. *Br. J. Pharmacol.* **119**, 1491–1497 (1996).
36. S. Vangveravong, M. Taylor, J. Xu, J. Cui, W. Calvin, S. Babic, R. R. Luedtke, R. H. Mach, Synthesis and characterization of selective dopamine D_2 receptor antagonists. 2. Azaindole, benzofuran, and benzothiophene analogs of L-741,626. *Bioorg. Med. Chem.* **18**, 5291–5300 (2010).
37. D. F. Manvich, A. K. Petko, R. C. Branco, S. L. Foster, K. A. Porter-Stransky, K. A. Stout, A. H. Newman, G. W. Miller, C. A. Paladini, D. Weinshenker, Selective D_2 and D_3 receptor antagonists oppositely modulate cocaine responses in mice via distinct postsynaptic mechanisms in nucleus accumbens. *Neuropsychopharmacology* **44**, 1445–1455 (2019).
38. D. Thompson, M. Pusch, J. L. Whistler, Changes in G protein-coupled receptor sorting protein affinity regulate postendocytic targeting of G protein-coupled receptors. *J. Biol. Chem.* **282**, 29178–29185 (2007).
39. J. L. Whistler, J. Enquist, A. Marley, J. Fong, F. Gladher, P. Tsuruda, S. R. Murray, M. Von Zastrow, Modulation of postendocytic sorting of G protein-coupled receptors. *Science* **297**, 615–620 (2002).
40. A. C. Hanyaloglu, M. von Zastrow, Regulation of GPCRs by endocytic membrane trafficking and its potential implications. *Annu. Rev. Pharmacol. Toxicol.* **48**, 537–568 (2008).
41. A. Marchese, M. M. Paing, B. R. S. Temple, J. Trejo, G protein-coupled receptor sorting to endosomes and lysosomes. *Annu. Rev. Pharmacol. Toxicol.* **48**, 601–629 (2008).
42. K. Kuramoto, N. Wang, Y. Fan, W. Zhang, F. J. Schoenen, K. J. Frankowski, J. Marugan, Y. Zhou, S. Huang, C. He, Autophagy activation by novel inducers prevents BECN2-mediated drug tolerance to cannabinoids. *Autophagy* **12**, 1460–1471 (2016).
43. R. J. Platt, S. Chen, Y. Zhou, M. J. Yim, L. Swiech, H. R. Kempton, J. E. Dahlman, O. Parnas, T. M. Eisenhaure, M. Jovanovic, D. B. Graham, S. Jhunjhunwala, M. Heidenreich, R. J. Xavier, R. Langer, D. G. Anderson, N. Hacohen, A. Regev, G. Feng, P. A. Sharp, F. Zhang, CRISPR-Cas9 knockin mice for genome editing and cancer modeling. *Cell* **159**, 440–455 (2014).
44. T. E. Robinson, K. C. Berridge, The neural basis of drug craving: An incentive-sensitization theory of addiction. *Brain Res. Brain Res. Rev.* **18**, 247–291 (1993).

45. D. F. Egan, M. G. H. Chun, M. Vamos, H. Zou, J. Rong, C. J. Miller, H. J. Lou, D. Raveendra-Panickar, C.-C. Yang, D. J. Sheffler, P. Teriete, J. M. Asara, B. E. Turk, N. D. P. Cosford, R. J. Shaw, Small molecule inhibition of the autophagy kinase ULK1 and identification of ULK1 substrates. *Mol. Cell* **59**, 285–297 (2015).
46. N. Hosokawa, T. Hara, T. Kaizuka, C. Kishi, A. Takamura, Y. Miura, S.-i. Iemura, T. Natsume, K. Takehana, N. Yamada, J.-L. Guan, N. Oshiro, N. Mizushima, Nutrient-dependent mTORC1 association with the ULK1-Atg13-FIP200 complex required for autophagy. *Mol. Biol. Cell* **20**, 1981–1991 (2009).
47. J. Kim, M. Kundu, B. Viollet, K.-L. Guan, AMPK and mTOR regulate autophagy through direct phosphorylation of Ulk1. *Nat. Cell Biol.* **13**, 132–141 (2011).
48. J. Liu, H. Xia, M. Kim, L. Xu, Y. Li, L. Zhang, Y. Cai, H. V. Norberg, T. Zhang, T. Furuya, M. Jin, Z. Zhu, H. Wang, J. Yu, Y. Li, Y. Hao, A. Choi, H. Ke, D. Ma, J. Yuan, Beclin1 controls the levels of p53 by regulating the deubiquitination activity of USP10 and USP13. *Cell* **147**, 223–234 (2011).
49. J.-M. Wong, P. A. Malec, O. S. Mabrouk, J. Ro, M. Dus, R. T. Kennedy, Benzoyl chloride derivatization with liquid chromatography-mass spectrometry for targeted metabolomics of neurochemicals in biological samples. *J. Chromatogr. A* **1446**, 78–90 (2016).
50. S. B. Caine, S. S. Negus, N. K. Mello, S. Patel, L. Bristow, J. Kulagowski, D. Vallone, A. Saiardi, E. Borrelli, Role of dopamine D2-like receptors in cocaine self-administration: Studies with D2 receptor mutant mice and novel D2 receptor antagonists. *J. Neurosci.* **22**, 2977–2988 (2002).
51. J. Boeuf, J. M. Trigo, P.-H. Moreau, L. Lecourtier, E. Vogel, J.-C. Cassel, C. Mathis, P. Klosen, R. Maldonado, F. Simonin, Attenuated behavioural responses to acute and chronic cocaine in GASP-1-deficient mice. *Eur. J. Neurosci.* **30**, 860–868 (2009).
52. D. Thompson, L. Martini, J. L. Whistler, Altered ratio of D1 and D2 dopamine receptors in mouse striatum is associated with behavioral sensitization to cocaine. *PLOS ONE* **5**, e11038 (2010).
53. Y. Yan, A. H. Newman, M. Xu, Dopamine D1 and D3 receptors mediate reconsolidation of cocaine memories in mouse models of drug self-administration. *Neuroscience* **278**, 154–164 (2014).
54. J. K. Shepherd, S. S. Grewal, A. Fletcher, D. J. Bill, C. T. Dourish, Behavioural and pharmacological characterisation of the elevated "zero-maze" as an animal model of anxiety. *Psychopharmacology (Berl)* **116**, 56–64 (1994).
55. Y. Li, Q. Kong, J. Yue, X. Gou, M. Xu, X. Wu, Genome-edited skin epidermal stem cells protect mice from cocaine-seeking behaviour and cocaine overdose. *Nat. Biomed. Eng.* **3**, 105–113 (2019).
56. P. R. Dunkley, P. E. Jarvie, P. J. Robinson, A rapid Percoll gradient procedure for preparation of synaptosomes. *Nat. Protoc.* **3**, 1718–1728 (2008).
57. M. K. Bermejo, M. Milenkovic, A. Salahpour, A. J. Ramsey, Preparation of synaptic plasma membrane and postsynaptic density proteins using a discontinuous sucrose gradient. *J. Vis. Exp.*, e51896 (2014).
58. A. K. Finn, J. L. Whistler, Endocytosis of the mu opioid receptor reduces tolerance and a cellular hallmark of opiate withdrawal. *Neuron* **32**, 829–839 (2001).
59. K. W. Dunn, M. M. Kamocka, J. H. McDonald, A practical guide to evaluating colocalization in biological microscopy. *Am. J. Physiol. Cell Physiol.* **300**, C723–C742 (2011).
60. F. Gaven, P. Marin, S. Claeysen, Primary culture of mouse dopaminergic neurons. *J. Vis. Exp.*, e51751 (2014).

Acknowledgments: We thank A. Belmadani for assistance with stereotaxic surgery, C. Horbinski for assistance with DA neuron integrity analysis, K. Sadleir for assistance with tissue sectioning, the Behavioral Phenotyping Core and the NUSeq Core of Center for Genetic Medicine at Northwestern University for technical support and assistance, and J. Whistler at the University of California at Davis for the Flag-D2R HEK293 stable cell line. **Funding:** Y.-J.K., S.Y., K.K., N.W., J.H.H., X.Q., and C.H. were supported by NIH R01-DK113170 (to C.H.), the BrightFocus Foundation (to C.H.), and Northwestern University startup funds (to C.H.). M.X. was supported by NIH R01-DA047785, NIH R21-AA027172, and NIH R01-DA043361. Y.Z. was supported by the Research Grants Council of Hong Kong Grant PolyU 151015/17M. H.D. was supported by NIH R01-MH109466. H.Y.M. was supported by the Weisman Family Foundation and Northwestern Memorial Foundation. **Author contributions:** Y.-J.K. and C.H. conceived the project and designed the experiments. Y.-J.K., Q.K., S.Y., K.K., N.W., M.H., J.H.H., T.X., and X.Q. performed the experiments. Y.-J.K., Q.K., S.Y., and C.H. analyzed the data. Y.Z., R.J.M., H.D., H.Y.M., and M.X. provided expertise. B.L. provided feedback. Y.-J.K., Q.K., M.X., and C.H. wrote the manuscript. **Competing interests:** The authors declare that they have no competing interests. **Data and materials availability:** All data needed to evaluate the conclusions in the paper are present in the paper and/or the Supplementary Materials. Additional data related to this paper may be requested from the authors.

Submitted 16 May 2020
Accepted 6 January 2021
Published 19 February 2021
10.1126/sciadv.abc8310

Citation: Y.-J. Kim, Q. Kong, S. Yamamoto, K. Kuramoto, M. Huang, N. Wang, J. H. Hong, T. Xiao, B. Levine, X. Qiu, Y. Zhao, R. J. Miller, H. Dong, H. Y. Meltzer, M. Xu, C. He, An autophagy-related protein Becn2 regulates cocaine reward behaviors in the dopaminergic system. *Sci. Adv.* **7**, eabc8310 (2021).

Science Advances

An autophagy-related protein Becn2 regulates cocaine reward behaviors in the dopaminergic system

Yoon-Jin Kim, Qingyao Kong, Soh Yamamoto, Kenta Kuramoto, Mei Huang, Nan Wang, Jung Hwa Hong, Tong Xiao, Beth Levine, Xianxiu Qiu, Yanxiang Zhao, Richard J. Miller, Hongxin Dong, Herbert Y. Meltzer, Ming Xu and Congcong He

Sci Adv **7** (8), eabc8310.
DOI: 10.1126/sciadv.abc8310